ELSEVIER

Coordination Chemistry Reviews
200–202 (2000) 563–594

COORDINATION CHEMISTRY REVIEWS

www.elsevier.com/locate/ccr

Quantification of isomeric equilibria for metal ion complexes formed in solution by phosphate or phosphonate ligands with a weakly coordinating second site

Helmut Sigel *, Larisa E. Kapinos

University of Basel, Institute of Inorganic Chemistry, Spitalstrasse 51, CH-4056 Basel, Switzerland

Received 5 November 1999; accepted 26 January 2000

Contents

* Corresponding author. Fax: +41-61-2671017.
E-mail address: helmut.sigel@unibas.ch (H. Sigel).

PII: S0010-8545(00)00307-6

Abstract

Weakly coordinating binding sites of ligands may give rise in their metal ion complexes in solution to intramolecular equilibria between an 'open' and a 'closed' form; 'closed' form meaning that a metal ion is bound to a strongly ligating group, which largely determines the overall stability of the complex, and in addition to a weakly coordinating site. This article describes how intramolecular equilibria of the indicated kind can be quantified. For complexes formed by Mg^{2+}, Ca^{2+}, Sr^{2+}, Ba^{2+}, Mn^{2+}, Co^{2+}, Ni^{2+}, Cu^{2+}, Zn^{2+} or Cd^{2+} and the dianion of (phosphonomethoxy)ethane, dihydroxyacetone phosphate, glycerol 1-phosphate, acetyl phosphate or acetonylphosphonate the intramolecular equilibria are evaluated and it is shown that oxygen atoms of ether, hydroxy or carbonyl groups can participate in metal ion binding, the extent of which being dependent on the metal ion involved. A decrease of the solvent polarity (e.g. by the addition of 1,4-dioxane to an aqueous solution) favors these weak oxygen–metal ion interactions, which are, of course, connected with some increase in stability. A stability increase of 0.1 log unit already means a formation degree of 20% of the closed isomer, yet the change in free energy is very small, i.e. $\Delta G° = -0.57$ kJ mol^{-1}. The importance of such weak interactions for the reaction processes occurring in the active-site cavities of enzymes is emphasized. For the complexes formed between the metal ions mentioned and flavin mononucleotide (FMN^{2-}) stability increases of about 0.1–0.2 log units are observed compared to the expected complex stabilities based on the basicity of the phosphate group. This increased stability is not attributed to a specific interaction with a weakly coordinating site but rather to a hydrophobic influence of the bulky isoalloxazine residue reducing in a 'folded' form the 'effective' dielectric constant in the microenvironment of the metal ion. Finally, weakly binding O and N sites behave differently under conditions of a reduced solvent polarity allowing nature to discriminate under such conditions between these kind of sites.

Keywords: Carbonyl oxygen ligating sites; Ether oxygen ligating sites; Intramolecular isomeric equilibria; Phosphate monoesters; Phosphonate derivatives

1. Introduction

Derivatives of orthophosphoric acid, mainly esters and anhydrides, occur widely in living systems [1] and they are involved in many metabolic events which also involve metal ions [2]. Well known examples are nucleoside mono-, di- and tri-phosphates as well as nucleic acids, in which the phosphate groups are important binding sites for metal ions [3–5]. Thus, it is not surprising that nucleotide–metal ion interactions have received considerable attention [4] and much, yet not enough [6], information exists about the stabilities [7–10] and properties [6,11–13] of such complexes in solution. This is quite different if one considers other phosphate esters and anhydrides such as, e.g. alanyl ethyl phosphate, the mixed anhydride of alanine

and phosphoric acid, the hydrolysis of which is promoted by metal ions [14]. Indeed, mixed-acid anhydrides occur widely in nature [15]; e.g. aminoacyl adenylates have a role in protein synthesis [16].

An intriguing question one is often confronted with in dealing with compounds of the last mentioned type concerns the participation of hydroxy, ether or carbonyl oxygen atoms in metal ion-binding processes involving, e.g. Ca^{2+}, Mg^{2+} or Zn^{2+}. Therefore, in this article we are summarizing and discussing the properties of a few such compounds which have been studied in solution in relatively great detail, and these results should then allow extrapolations to other related systems. The ligands considered are shown in Fig. 1; all of them are of biological relevance as is shortly indicated below.

Since nucleotides lie at the crossroad of many metabolic processes [2,3], attempts to produce therapeutically useful nucleotide derivatives are longstanding [17]. So-called acyclic-nucleoside phosphonates [18] represent a structural class of such derivatives; they are analogues of (2′-deoxy)nucleoside 5′-monophosphates in which the ribose-phosphate residue is replaced by an aliphatic chain with a phosphonate group. Indeed, the nucleotide analogues with a (phosphonomethoxy)ethyl residue (see Fig. 3 in Section 3) are among the most promising novel compounds with antiviral properties [18,19]. For this reason the nucleobase-free part of these analogues, i.e. (phosphonomethoxy)ethane (see Fig. 1(A)), deserves to be studied in detail with regard to its metal ion-binding properties. Indeed, it was shown [20] that the ether oxygen participates to some extent in metal ion coordination (see Section 3). Interestingly, this ether oxygen is also compulsory for an antiviral activity [21] and its importance for the correct location of metal ions during the facilitated synthesis of nucleic acids by polymerases was recently explained [22,23].

Dihydroxyacetone phosphate ($DHAP^{2-}$) and glycerol 1-phosphate ($G1P^{2-}$) (see Fig. 1(B)) are important intermediates in biological processes [15,24]. For example, the most important membrane lipids in many cells are constructed upon a backbone of glycerol 1-phosphate [15,25]. DHAP is next to glyceraldehyde 3-phosphate (GAP) produced in the catabolism of glucose which proceeds via fructose-1,6-bisphosphate (FBP); the corresponding class II aldolase, a Zn^{2+} enzyme, catalyzes the cleavage of FBP into DHAP and GAP as well as the reverse condensation reaction [26]; this enzyme utilizes in addition monovalent ions (Na^+, K^+, NH_4^+) [26]. The so-called α-glycerophosphate shuttle [15] transforming DHAP and G1P into each other is important for the synthesis of ATP [24], which also depends on the presence of Ca^{2+} [27]. The shuttle is depicted in a simplified way in Fig. 1(B); it occurs in tissues of many organisms including insect flight muscles [15,24].

A large number of enzymes employ acetyl phosphate (AcP^{2-}; see Fig. 1(C)) as substrate [28]. For example, AcP is able to phosphorylate an aspartate residue in the OmpR protein, which is part of the regulatory system of the porin gene expression in *Escherichia coli* [29]. However, one of the most prominent reactions of AcP is the formation of $Mg(ATP)^{2-}$ via $Mg(ADP)^-$ by activating acetate with acetyl coenzyme A synthetase and synthesizing from acetyl coenzyme A with phosphotransacetylase AcP which then, with an acetate kinase, provides ATP and acetate [30,31]. Indeed, it was concluded that acetyl phosphate is the best phosphate

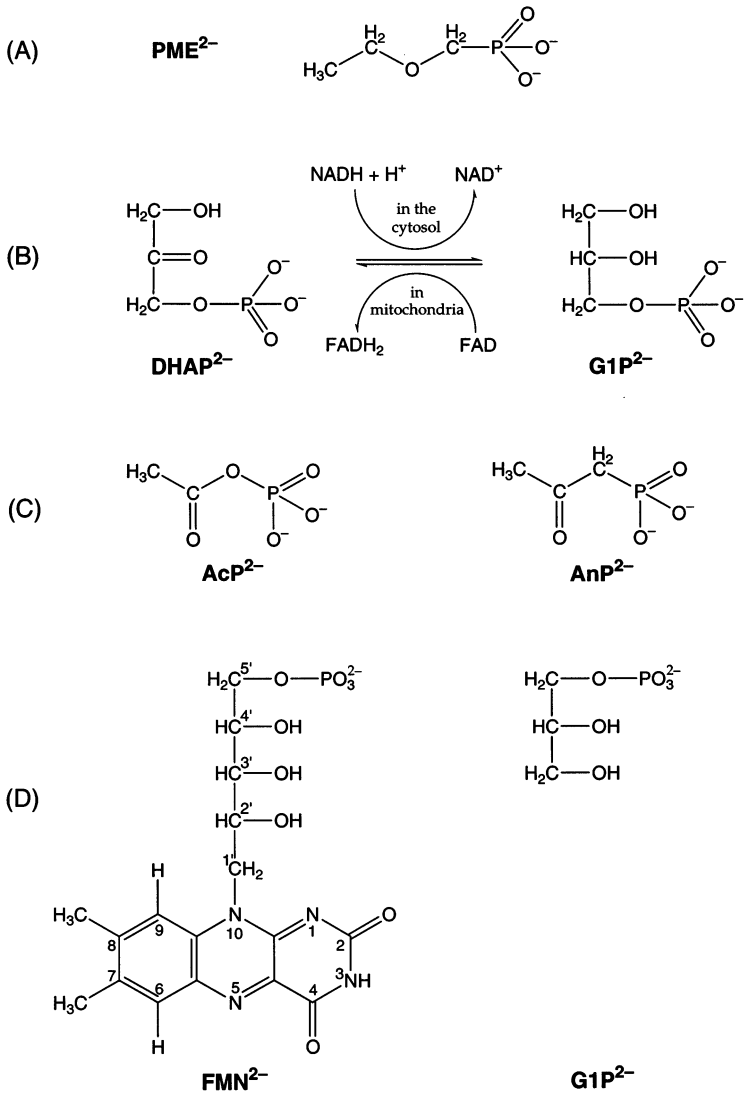

Fig. 1. Chemical structures of the phosphate and phosphonate derivatives considered in this article as ligands: (**A**) Dianion of (phosphonomethoxy)ethane (PME^{2-} = ethoxymethanephosphonate); see Section 3. (**B**) Simplified representation of the so-called [15] α-glycerophosphate shuttle in which dihydroxyacetone phosphate ($DHAP^{2-}$) and glycerol 1-phosphate ($G1P^{2-}$) are interconverted into each other [15,24]. In the experiments summarized in Section 4 D,L-G1P was used but this is without consequences for the comparisons made herein. (**C**) Acetyl phosphate (AcP^{2-}) and acetonylphosphonate (AnP^{2-}); see Section 5. (**D**) Flavin mononucleotide (FMN^{2-} = riboflavin 5′-phosphate) together with glycerol 1-phosphate ($G1P^{2-}$) depicted again to emphasize the structural identity with a part of the FMN^{2-} ligand; see Section 6.

donor to synthesize ATP [32] for commercial processes. Similarly, γ-labeled nucleoside 5′-triphosphates are easy to prepare with [^{32}P]acetyl phosphate and acetate kinase [33]. The AcP analogue, acetonylphosphonate (AnP^{2-}; Fig. 1(C)) which is hydrolysis-stable, has been employed, e.g. as an inhibitor of various enzyme systems [34]. However, AnP is also a substrate for the P–C bond-cleaving enzyme phosphonoacetaldehyde hydrolase, where it undergoes enzyme-catalyzed hydrolysis to hydrogen phosphate and acetone [35].

Flavin mononucleotide (FMN^{2-}; see Fig. 1(D)), also known as riboflavin 5′-phosphate, is together with flavin adenine dinucleotide (FAD^{2-}), the coenzyme of a large number of enzymes which catalyze various redox reactions in biological systems [15,16,24]; their properties have been [36], and still are, extensively studied [37–41]. The metal ion-binding properties of FMN^{2-} are of interest, because many of the FMN-dependent enzymes contain also molybdenum and/or iron [24,36–41]. In these multicenter redox proteins, iron is present in heme groups [38–40] or iron–sulfur clusters [41]. A great number of such enzymes are known and more are still being discovered or are described in greater detail [37–41]; in fact, in various instances Ca^{2+} is also involved in the reaction processes [39,42] and, e.g. the biosynthesis of nitric oxide (NO) by the enzyme NO synthase, a relatively complicated reaction which includes several protein-bound cofactors, also depends on FMN [38–40].

2. Isomeric equilibria in complexes involving, next to a strong, a weakly coordinating binding site. General considerations

The present considerations are restricted to complexes in solution, involving the alkaline earth ions and the divalent ions of the second half of the 3d series as well as Zn^{2+} and Cd^{2+}. A view of the ligand structures depicted in Fig. 1 reveals immediately that in all instances the twofold negatively charged phosph(on)ate residue is the main binding site for all the mentioned metal ions, especially for those of prime biological interest, Ca^{2+} [43], Mg^{2+} [44], Mn^{2+} [45], and Zn^{2+} [46]. Consequently, the phosph(on)ate residue will determine to a large degree the stability of the corresponding complexes, but next to this primary binding site, the oxygen atoms of the ether, hydroxy, carbonyl, etc., groups might also possibly participate in metal ion binding. If so, this would give rise in solution to the intramolecular equilibrium (1):

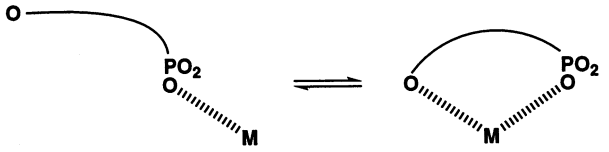

(1)

Of course, any participation in metal ion binding of one of these weakly coordinating sites must still be reflected to some extent in the overall stability of the complexes [47].

The position of the concentration-independent equilibrium (1) between an 'open' isomer, ML_{op}, and a chelated or 'closed' species involving the more weakly binding O atom, ML_{cl}, is defined by the intramolecular and hence, dimensionless, equilibrium constant K_I:

$$K_I = [ML_{cl}]/[ML_{op}] \tag{2}$$

In Eq. (2) as well as in all the following equations L^{2-} represents PME^{2-}, $DHAP^{2-}$, $G1P^{2-}$, AcP^{2-}, AnP^{2-}, or FMN^{2-} (see Fig. 1).

Usually, the stability constants of 1:1 complexes measured experimentally are defined as given in Eq. (3):

$$M^{2+} + L^{2-} \rightleftharpoons ML \tag{3a}$$

$$K^{M}_{ML} = [ML]/([M^{2+}][L^{2-}]) \tag{3b}$$

This means that [ML] represents the sum of the concentrations of all ML isomers present. Clearly, due to equilibrium (1) the expressions (3a,b) may be rewritten as given in Eqs. (4) and (5):

$$M^{2+} + L^{2-} \rightleftharpoons ML_{op} \rightleftharpoons ML_{cl} \tag{4}$$

$$K^{M}_{ML} = \frac{([ML_{op}] + [ML_{cl}])}{[M^{2+}][L^{2-}]} \tag{5a}$$

$$= \frac{[ML_{op}]}{[M^{2+}][L^{2-}]} + \frac{[ML_{cl}]}{[M^{2+}][L^{2-}]} \tag{5b}$$

From Eqs. (2) and (5) follow [47,48] Eqs. (6) and (7):

$$K^{M}_{ML} = K^{M}_{ML_{op}} + K^{M}_{ML_{cl}} \tag{6a}$$

$$= K^{M}_{ML_{op}}(1 + K_I) \tag{6b}$$

$$K_I = \frac{K^{M}_{ML}}{K^{M}_{ML_{op}}} - 1 = 10^{\log \Delta} - 1 \tag{7}$$

Of course, in deriving Eq. (6), the definition of Eq. (2) as well as that for the stability constant of the open isomer, $K^{M}_{ML_{op}}$ (Eq. (8)), was used.

$$K^{M}_{ML_{op}} = [ML_{op}]/([M^{2+}][L^{2-}]) \tag{8}$$

The stability constant of the open isomer (Eq. (8)) is not directly accessible by experiments, yet it may be calculated with the acidity constant, K^{H}_{HL} (Eq. (9)),

$$K^{H}_{HL} = [H^{+}][L^{2-}]/[HL^{-}] \tag{9}$$

which is due to the deprotonation of the $-P(O)_2(OH)^-$ residue in HL^- together with the equations of the correlation lines for $\log K^{M}_{ML}$ versus pK^{H}_{HL} plots. These are listed in Table 1 [49–54] for the ten metal ions already mentioned as well as for three different solvents. In addition, the straight reference-line equations are given for mixed ligand systems containing 2,2′-bipyridine (Bpy) or 1,10-phenanthroline (Phen), i.e. for Cu(Bpy)L and Cu(Phen)L (entries 11, 12, 14, and 16 of Table 1).

These plots were constructed with simple phosphonate [49] or phosphate monoester [50] ligands with a non-coordinating residue, like phenyl phosphate or *n*-butyl phosphate (see the legend for Fig. 2 in Section 3). As one would expect, the equilibrium data for the simple methanephosphonate and ethanephosphonate ligands also fit on these straight lines (see also Fig. 2, vide infra). Hence, with this procedure $\log K^{M}_{ML_{op}}$ is obtained and thus, the stability-constant difference according to Eq. (10)

$$\log \Delta = \log \Delta_{ML} = \log K^{M}_{ML_{exper}} - \log K^{M}_{ML_{calc}} \quad (10a)$$

$$= \log K^{M}_{ML} - \log K^{M}_{ML_{op}} = \log(1 + E) \quad (10b)$$

Table 1
Straight-line correlations for M^{2+}-phosphate monoester or -phosphonate complex stabilities and phosph(on)ate group basicities[a]

No.	% (v/v) dioxane	M^{2+}	*m*	*b*	S.D.
1	0	Mg^{2+}	0.208 ± 0.015	0.272 ± 0.097	0.033
2	0	Ca^{2+}	0.131 ± 0.020	0.636 ± 0.131	0.048
3	0	Sr^{2+}	0.082 ± 0.016	0.732 ± 0.102	0.036
4	0	Ba^{2+}	0.087 ± 0.016	0.622 ± 0.107	0.039
5	0	Mn^{2+}	0.238 ± 0.022	0.683 ± 0.144	0.051
6	0	Co^{2+}	0.223 ± 0.026	0.554 ± 0.167	0.057
7	0	Ni^{2+}	0.245 ± 0.023	0.422 ± 0.147	0.051
8	0	Cu^{2+}	0.465 ± 0.025	−0.015 ± 0.164	0.057
9	0	Zn^{2+}	0.345 ± 0.026	−0.017 ± 0.171	0.060
10	0	Cd^{2+}	0.329 ± 0.019	0.399 ± 0.127	0.045
11	0	$Cu(Bpy)^{2+}$	0.465	0.009	0.066
12	0	$Cu(Phen)^{2+}$	0.465	0.018	0.063
13	30	Cu^{2+}	0.559 ± 0.015	−0.089 ± 0.106	0.03
14	30	$Cu(Bpy)^{2+}$	0.559	−0.007	0.039
15	50	Cu^{2+}	0.571 ± 0.022	0.190 ± 0.160	0.03
16	50	$Cu(Bpy)^{2+}$	0.571	0.334	0.069

[a] Slopes (*m*) and intercepts (*b*) for the straight-base-line plots of $\log K^{M}_{ML}$ (Eq. (3b)) versus pK^{H}_{HL} (Eq. (9)) (see Figs. 2 and 4–6) as calculated by the least-squares procedure from the equilibrium constants for simple $R\text{-}PO_3^{2-}/H^+/M^{2+}$ systems (R = non-coordinating residue)[b] obtained in aqueous solutions and in water containing 30 or 50% (v/v) 1,4-dioxane at 25°C and $I = 0.1$ M ($NaNO_3$)[c,d].

[b] $L^{2-} = R\text{-}PO_3^{2-}$ = 4-nitrophenyl phosphate, phenyl phosphate, *n*-butyl phosphate, D-ribose-5-monophosphate, uridine 5′-monophosphate, thymidine 5′-monophosphate, methanephosphonate and ethanephosphonate (see legend for Fig. 2) [49,50]; in the mixed solvents and in the ternary systems not all ligands were studied (see Fig. 4) [51–53].

[c] Straight-line equation: $y = m \cdot x + b$, where *x* represents the pK^{H}_{HL} value of any monoprotonated phosph(on)ate group and *y* the calculated stability constant ($\log K^{M}_{ML}$) of the corresponding ML complex; the errors given with *m* and *b* correspond to one standard deviation (1σ). The column at the right lists three times the standard deviations (S.D.) resulting from the differences between the experimental and calculated values for the mentioned[b] ligand systems. The listed S.D. values (3σ) are considered as reasonable error limits for any stability constant calculation in the pK^{H}_{HL} range 5–8 for aqueous solution, 6–8.5 for 30%, and 6.5–9 for 50% (v/v) dioxane–water mixtures.

[d] Entries 1–10 are from Tables 5 and 6 in Ref. [49], entries 11 and 12 from Table 5 of Ref. [51], entries 13 and 15 from Table 2 of Ref. [52] (see also Table 2 in Ref. [54]), and entries 14, and 16 from Table 2 of Ref. [53].

can be calculated, which then also defines the second term in Eq. (7) above. It may be added that the value for $10^{\log \Delta}$ is sometimes also addressed as the stability enhancement factor $(1 + E)$ [47]. Finally, the correspondence of the terms appearing in the differences of Eqs. (10a) and (10b) is evident.

Clearly, the reliability of any calculation for K_I (Eqs. (2) and (7)) depends on the accuracy of the difference $\log \Delta_{ML}$, which becomes the more important the more similar the two constants in Eq. (10b) are. Therefore, only well-defined error limits allow a quantitative evaluation of the position of equilibrium (1). Finally, if K_I is known, the percentage of the closed or chelated isomer occurring in equilibrium (1) follows from equation (11):

$$\%ML_{cl} = 100 \cdot K_I/(1 + K_I) \quad (11)$$

Application of this procedure [47,48] yields the results listed in the various tables of Sections 3–6.

3. Complexes of the anionic (phosphonomethoxy)ethane ligand (PME^{2-}). The ether oxygen participates in metal ion coordination!

The dianion of (phosphonomethoxy)ethane (PME^{2-}; see Fig. 1(A)) is a relatively simple ligand, since any possibly observed increased stability beyond that expected for the phosphonate group has to be attributed to the ether oxygen alone because no other potential binding site is present. For this reason we begin our survey with the M^{2+} complexes of PME^{2-}.

Fig. 2 shows plots of $\log K^{M}_{ML}$ versus pK^{H}_{HL} for the 1:1 complexes of Ca^{2+}, Co^{2+}, and Cd^{2+} with eight simple ligands (see legend of Fig. 2) allowing only a phosph(on)ate–M^{2+} interaction [49,50]. The corresponding least-squares reference lines, the parameters of which are listed in Table 1 of Section 2, define the relation between phosph(on)ate-complex stability and phosph(on)ate-group basicity. The three solid circles in Fig. 2, which refer to Ca(PME), Co(PME), and Cd(PME), are considerably above their reference lines [49], thus proving an increased stability for these complexes.

A quantitative evaluation of the situation reflected in Fig. 2 is possible by calculating with $pK^{H}_{H(PME)}$ and the straight-line equations of Table 1 the expected stabilities for the M(PME) complexes with a sole phosphonate-M^{2+} coordination, i.e. for the $M(PME)_{op}$ species. The corresponding results are listed in column 5 of Table 2; their comparison according to Eq. (10) with the measured stability constants (column 4) lead to the stability differences given in the sixth column of Table 2. Evidently all the M(PME) complexes are more stable than expected on the basis of the basicity of the PME^{2-}-phosphonate group.

As indicated in Section 2, any increased stability must be attributed [47] to a further metal ion interaction; i.e. in the present case to the ether oxygen. Conse-

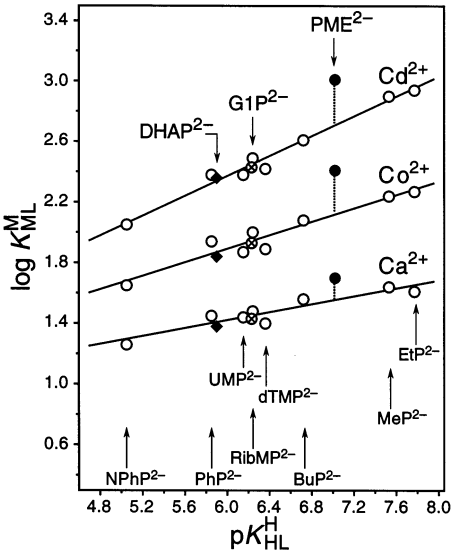

Fig. 2. Evidence for an enhanced stability of some M(PME) (●) complexes, based on the relationship between $\log K^{M}_{ML}$ and pK^{H}_{HL} for the 1:1 complexes of Ca^{2+}, Co^{2+}, and Cd^{2+} with some simple phosphate monoester or phosphonate ligands: 4-nitrophenyl phosphate ($NPhP^{2-}$), phenyl phosphate (PhP^{2-}), uridine 5′-monophosphate (UMP^{2-}), D-ribose 5-monophosphate ($RibMP^{2-}$), thymidine [1-(2′-deoxy-β-D-ribofuranosyl)thymine] 5′-monophosphate ($dTMP^{2-}$), *n*-butyl phosphate (BuP^{2-}), methanephosphonate (MeP^{2-}), and ethanephosphonate (EtP^{2-}) (from left to right) (○). The least-squares lines are drawn through the corresponding eight data sets [49,50]; the equations for these base lines are given in Table 1 (entries 2, 6 and 10). The vertical broken lines emphasize the stability differences of the M(PME) (●) complexes to the corresponding reference lines; these differences are equal to $\log \Delta_{M(PME)}$ (Eq. (10)), the values of which are listed in column 6 of Table 2. The equilibrium constants for the data points due to the PME systems are taken from Tables 1 and 8 of Ref. [49] (see also Table 2). For further comparison also the data points for the DHAP (◆) and G1P (⊗) systems, to be discussed in Section 4.1 (Table 4 [61]), are inserted into this figure. All plotted equilibrium constant values refer to aqueous solutions at 25°C and $I = 0.1$ M ($NaNO_3$).

quently, five-membered chelates, $M(PME)_{cl}$, must be formed to some extent and thus, equilibrium (12) operates.

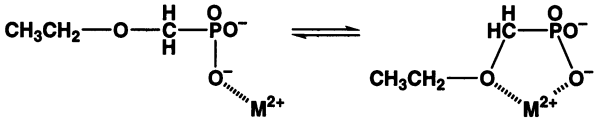

(12)

Application of the evaluation procedure described in Section 2 and defined by Eqs. (7), (10) and (11) gives the results summarized in Table 3. It is evident that for all the complexes studied at least some chelate formation occurs; indeed, the formation degree varies between about 15 and 75%.

From entries 1–10 in Table 3 follows that in aqueous solution all alkaline metal ions and all ions of the second half of the 3d series as well as Zn^{2+} and Cd^{2+} form chelates. For Fe(PME) no values are given, since experiments with Fe^{2+} are difficult to carry out [6a], but it is safe to assume (cf. Ref. [6a]) that the data for

Fe(PME) are close to the average of the results obtained for Mn(PME) and Co(PME). Chelate formation persists in aqueous solutions containing 1,4-dioxane, as is evident from entries 14–16 of Table 3; in fact, it appears that the formation degree of $Cu(PME)_{cl}$ is hardly affected by the reduction of the polarity of the solvent (cf. also Table 5 in Section 4.2). There might be a hint that increasing amounts of 1,4-dioxane slightly inhibit chelate formation; in any case, it is *not* favored as it is the case with $DHAP^{2-}$ and $G1P^{2-}$ complexes (see Section 4.2).

A slight inhibition of $Cu(PME)_{cl}$ by 1,4-dioxane is feasible, as hydrophobic solvation of the ethyl residue of PME^{2-} by the ethylene bridges of 1,4-dioxane will hinder the ether oxygen coordination. This notion is confirmed by the properties of the mixed ligand complexes with 2,2′-bipyridine and 1,10-phenanthroline for which a slight increase in the formation degree in aqueous solution is observed (entries 11–13 of Table 3) and this has tentatively been attributed [53] to a weak hydrophobic interaction between the terminal ethyl residue of PME^{2-} and an edge of the

Table 2
Comparison of the measured stability constants, $K^{M}_{M(PME)}$ (Eqs. (3)–(5)), of the M(PME) complexes with the calculated stability constants for the open isomers with a sole phosphonate–M^{2+} coordination, $K^{M}_{ML_{(PME)_{op}}}$ (Eq. (8)); the observed stability increase is expressed by log $\Delta_{M(PME)}$ (Eq. (10))[a–d]

No.	% (v/v) dioxane	M^{2+}	log $K^{M}_{M(PME)}$	log $K^{M}_{M(PME)_{op}}$[e]	log $\Delta_{M(PME)}$
1	0	Mg^{2+}	1.95 ± 0.01	1.73 ± 0.03	0.22 ± 0.03
2	0	Ca^{2+}	1.70 ± 0.01	1.56 ± 0.05	0.14 ± 0.05
3	0	Sr^{2+}	1.38 ± 0.03	1.31 ± 0.04	0.07 ± 0.05
4	0	Ba^{2+}	1.33 ± 0.03	1.23 ± 0.04	0.10 ± 0.05
5	0	Mn^{2+}	2.62 ± 0.02	2.35 ± 0.05	0.27 ± 0.05
6	0	Co^{2+}	2.41 ± 0.02	2.12 ± 0.06	0.29 ± 0.06
7	0	Ni^{2+}	2.33 ± 0.02	2.14 ± 0.05	0.19 ± 0.05
8	0	Cu^{2+}	3.73 ± 0.03	3.25 ± 0.06	0.48 ± 0.07
9	0	Zn^{2+}	2.74 ± 0.02	2.40 ± 0.06	0.34 ± 0.06
10	0	Cd^{2+}	3.01 ± 0.02	2.71 ± 0.05	0.30 ± 0.05
11	0	Cu^{2+}	3.73 ± 0.03	3.25 ± 0.06	0.48 ± 0.07
12	0	$Cu(Bpy)^{2+}$	3.86 ± 0.03	3.27 ± 0.07	0.59 ± 0.08
13	0	$Cu(Phen)^{2+}$	3.90 ± 0.04	3.28 ± 0.06	0.62 ± 0.07
14	0	Cu^{2+}	3.73 ± 0.03	3.25 ± 0.06	0.48 ± 0.07
15	30	Cu^{2+}	4.62 ± 0.03	4.23 ± 0.03	0.39 ± 0.04
16	50	Cu^{2+}	5.27 ± 0.06	4.86 ± 0.03	0.41 ± 0.07

[a] The data refer to aqueous solutions and to water containing 30 or 50% (v/v) 1,4-dioxane at 25°C and $I = 0.1$ M ($NaNO_3$).

[b] Entries 1–10 are taken from Table 8 of Ref. [49], entries 11–13 from Table 6 of Ref. [51], and entries 14–16 from Table 3 of Ref. [52].

[c] The acidity constants for $H(PME)^{-}$ in the various solvents are $pK^{H}_{H(PME)} = 7.02 \pm 0.01$ in water [49], as well as 7.73 ± 0.02 and 8.17 ± 0.03 in 30 and 50% (v/v) 1,4-dioxane, respectively [52][d].

[d] All equilibrium constants were measured by potentiometric pH titrations. All the errors given are three times the standard error of the mean value or the sum of the probable systematic errors, whichever is larger. The error limits of all derived data, e.g. log $\Delta_{M(PME)}$, were calculated according to the error propagation after Gauss.

[e] Calculated with the acidity constants $pK^{H}_{H(PME)}$ (see[c]) and the reference-line equations listed in Table 1; the error limits correspond to the S.D. values (3σ) given in Table 1.

Table 3
Extent of chelate formation according to the intramolecular equilibrium (12) in M(PME) complexes as quantified by the dimensionless equilibrium constant K_I (Eqs. (2) and (7)) and the percentage of the closed isomers, $M(PME)_{cl}$ (Eq. (11)) in water and in water containing 30 or 50% (v/v) 1,4-dioxane at 25°C and $I = 0.1$ M ($NaNO_3$)[a]

No.	% (v/v) dioxane	M^{2+}	log $\Delta_{M(PME)}$	K_I	% $M(PME)_{cl}$
1	0	Mg^{2+}	0.22 ± 0.03	0.66 ± 0.12	40 ± 4
2	0	Ca^{2+}	0.14 ± 0.05	0.38 ± 0.16	28 ± 9
3	0	Sr^{2+}	0.07 ± 0.05	0.17 ± 0.14	15 ± 10
4	0	Ba^{2+}	0.10 ± 0.05	0.26 ± 0.14	21 ± 9
5	0	Mn^{2+}	0.27 ± 0.05	0.86 ± 0.23	46 ± 7
6	0	Co^{2+}	0.29 ± 0.06	0.95 ± 0.28	49 ± 7
7	0	Ni^{2+}	0.19 ± 0.05	0.55 ± 0.19	35 ± 8
8	0	Cu^{2+}	0.48 ± 0.07	2.02 ± 0.47	67 ± 5
9	0	Zn^{2+}	0.34 ± 0.06	1.19 ± 0.32	54 ± 7
10	0	Cd^{2+}	0.30 ± 0.05	1.00 ± 0.25	50 ± 6
11	0	Cu^{2+}	0.48 ± 0.07	2.02 ± 0.47	67 ± 5
12	0	$Cu(Bpy)^{2+}$	0.59 ± 0.08	2.89 ± 0.68	74 ± 5
13	0	$Cu(Phen)^{2+}$	0.62 ± 0.07	3.17 ± 0.69	76 ± 4
14	0	Cu^{2+}	0.48 ± 0.07	2.02 ± 0.47	67 ± 5
15	30	Cu^{2+}	0.39 ± 0.04	1.45 ± 0.24	59 ± 4
16	50	Cu^{2+}	0.41 ± 0.07	1.57 ± 0.40	61 ± 6

[a] For the error limits see footnote 'd' of Table 2. The values in column 4, on which the calculations are based (Eq. (7)), are those of column 6 in Table 2; see also Table 8 in Ref. [49] (entries 1–10), Table 6 in Ref. [51] (entries 11–13), and Table 5 in Ref. [52] (entries 14–16).

aromatic-ring systems of the coordinated Bpy or Phen favoring thus somewhat the formation of the chelated isomers, $Cu(Bpy)(PME)_{cl}$ and $Cu(Phen)(PME)_{cl}$.

However, three more points regarding entries 11–16 in Tables 2 and 3 warrant mentioning. (i) A partial saturation of the coordination sphere of a metal ion does not prevent a metal ion–ether oxygen interaction as follows from entries 11–13. (ii) The fact that the absolute stability constants (Table 2, column 4, entries 11–13) are slightly higher for the mixed ligand Cu^{2+} complexes, compared with the binary one, is in accord with the general experience regarding the combination of heteroaromatic N-base/O-donor ligands [53,55–57]. (iii) Entries 14–16 of Table 2 reveal that a change of the solvent from water to water containing 50% 1,4-dioxane increases complex stability by about 1.5 log units (column 4) whereas the formation degree of the chelated $Cu(PME)_{cl}$ isomer is hardly affected by this change in the solvent (Table 3, column 6).

In conclusion, under all the conditions considered, the involvement of the ether oxygen in complex formation is quite significant, including the complexes of Ca^{2+}, Mg^{2+}, Mn^{2+}, and Zn^{2+}, for which the formation degree of $M(PME)_{cl}$ varies between about 30 and 55%. This observation is of relevance, since the (phosphonomethoxy)ethyl residue is an important part of the nucleotide analogues shown in Fig. 3 which have mostly antiviral properties [18,19]. Indeed, for the $PMEC^{2-}$ complexes of the cytidine 5′-monophosphate (CMP^{2-}) analogue the formation of

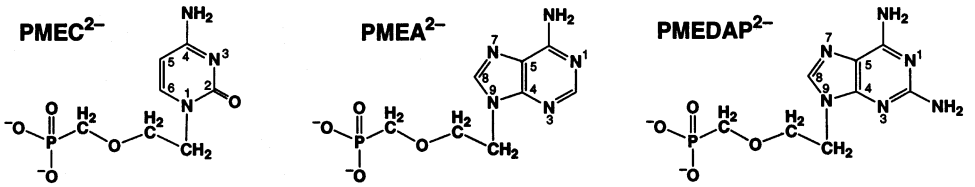

Fig. 3. Chemical structures of the dianions of 1-[2-(phosphonomethoxy)ethyl]cytosine ($PMEC^{2-}$), 9-[2-(phosphonomethoxy)ethyl]adenine ($PMEA^{2-}$), and 9-[2-(phosphonomethoxy)ethyl]-2,6-diaminopurine ($PMEDAP^{2-}$).

five-membered chelates analogous to equilibrium (12) has also been proven to occur [58]; that is, in the M(PMEC) complexes the cytosine residue does not participate in metal ion binding. This contrasts with the situation in the M(PMEA) and M(PMEDAP) complexes, the ligands of which can be considered as adenosine 5′-monophosphate (AMP^{2-}) analogues. Indeed, in certain M(PMEA) complexes, e.g. with Ni^{2+} and Cu^{2+}, in addition to the five-membered chelate of equilibrium (12) a seven-membered chelate involving N3 exists as a third isomer [22,59]. Interestingly, in M(PMEDAP) complexes N3 is no longer accessible for M^{2+} due to steric inhibition by the (C2)-NH_2 group, and therefore in these systems, next to the five-membered chelate, in equilibrium a macrochelate is formed as the third isomer by an interaction of the phosphonate-coordinated metal ion with N7 of the nucleobase residue [60]. However, for all the complexes of these nucleotide analogues (Fig. 3) equilibrium (12) is of importance and the relevance of the metal ion–ether oxygen coordination for the biological action of these compounds has recently been explained [22].

4. Stabilities of metal ion complexes formed with dihydroxyacetone phosphate ($DHAP^{2-}$) and glycerol 1-phosphate ($G1P^{2-}$)

The two ligands involved in the so-called α-glycerophosphate shuttle (see Fig. 1(B)) are both orthophosphate esters and they have a somewhat more complicated structure than PME^{2-} discussed in the preceding Section 3. Their potential additional binding sites, which are closest to the phosphate group are also of a different nature: $DHAP^{2-}$ offers a carbonyl oxygen and $G1P^{2-}$ a hydroxy group at C2 (Fig. 1(B)). Space-filling molecular models show that a phosphate-coordinated metal ion may also easily reach the carbonyl oxygen in M(DHAP) and, correspondingly, the hydroxy group in M(G1P). Hence, the question arises: does an equilibrium exist in solution between a solely phosphate-coordinated species and a seven-membered chelate? The corresponding equilibrium is indicated below in a simplified form, by neglecting the charges (Eq. (13)):

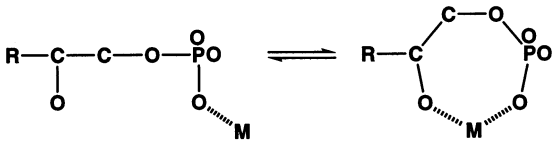

(13)

Of course, a metal ion coordinated to the phosphate group of $G1P^{2-}$ may equally well reach the 2-hydroxy group in the L or the D isomer: hence, the answer to the above question remains unaffected by the use of D,L-G1P in the previous study [61], which is reviewed here.

4.1. Studies in aqueous solution reveal a M^{2+}-phosphate coordination only!

The equilibrium constant values determined previously [61] for the Ca^{2+}, Co^{2+}, and Cd^{2+} complexes of $DHAP^{2-}$ and $G1P^{2-}$ are inserted in Fig. 2 which is part of Section 3. From this figure it is evident that the data pairs for the three mentioned systems clearly fall on their reference lines within the error limits; hence, there is no indication for an increased complex stability and thus equilibrium (13) lies on the left.

Indeed, by using the mentioned reference-line equations given in Table 1 and the pK^{H}_{HL} values of $H(DHAP)^{-}$ and $H(G1P)^{-}$ (Table 4), the logarithms of the stability

Table 4
Logarithms of the stability constants of M(DHAP) and M(G1P) complexes (Eqs. (3)–(5)) as determined by potentiometric pH titrations (Exp.) in aqueous solution at 25°C and $I = 0.1$ M ($NaNO_3$)[a]. The calculated stability constants for a pure and unaltered metal ion–phosphate residue coordination (Calc.), i.e. for ML_{op} (Eq. (8)), are given for comparison; these values are based on the straight-line equations quantifying the relationship between complex stability and phosphate-group basicity (see Table 1) and the pK^{H}_{HL} values[b] (Eq. (9)) of $H(DHAP)^{-}$ and $H(G1P)^{-}$. The stability differences according to Eq. (10) are also listed[c]

M^{2+}	log $K^{M}_{M(DHAP)}$		log $\Delta_{M(DHAP)}$	log $K^{M}_{M(G1P)}$		log $\Delta_{M(G1P)}$
	Exp.	Calc.		Exp.	Calc.	
Mg^{2+}	1.57 ± 0.03	1.50 ± 0.03	0.07 ± 0.04	1.63 ± 0.03	1.57 ± 0.03	0.06 ± 0.04
Ca^{2+}	1.38 ± 0.02	1.41 ± 0.05	-0.03 ± 0.05	1.43 ± 0.02	1.45 ± 0.05	-0.02 ± 0.05
Sr^{2+}	1.23 ± 0.03	1.22 ± 0.04	0.01 ± 0.05	1.23 ± 0.03	1.24 ± 0.04	-0.01 ± 0.05
Ba^{2+}	1.14 ± 0.09	1.14 ± 0.04	0.00 ± 0.10	1.18 ± 0.03	1.16 ± 0.04	0.02 ± 0.05
Mn^{2+}	2.11 ± 0.02	2.09 ± 0.05	0.02 ± 0.05	2.21 ± 0.04	2.17 ± 0.05	0.04 ± 0.06
Co^{2+}	1.84 ± 0.02	1.87 ± 0.06	-0.03 ± 0.06	1.93 ± 0.02	1.94 ± 0.06	-0.01 ± 0.06
Ni^{2+}	1.85 ± 0.03	1.87 ± 0.05	-0.02 ± 0.06	1.90 ± 0.04	1.95 ± 0.05	-0.05 ± 0.06
Cu^{2+}	2.77 ± 0.02	2.73 ± 0.06	0.04 ± 0.06	2.83 ± 0.05	2.88 ± 0.06	-0.05 ± 0.08
Zn^{2+}	2.01 ± 0.03	2.02 ± 0.06	-0.01 ± 0.07	2.13 ± 0.04	2.13 ± 0.06	0.00 ± 0.07
Cd^{2+}	2.36 ± 0.02	2.34 ± 0.05	0.02 ± 0.05	2.43 ± 0.03	2.45 ± 0.05	-0.02 ± 0.06

[a] These values (in columns 2 and 5) are taken from Table 2 in Ref. [61]. The other values listed in the table are revised compared to those given in Ref. [61].
[b] Acidity constants: $pK^{H}_{H(DHAP)} = 5.90 \pm 0.01$ and $pK^{H}_{H(G1P)} = 6.23 \pm 0.01$ [61].
[c] For the error limits see footnote 'd' of Table 2.

constants, $\log K^{M}_{ML_{op}}$, for the open isomers, $M(DHAP)_{op}$ and $M(G1P)_{op}$, can be calculated. These results are listed in columns 3 and 6 of Table 4. The differences between the measured and the calculated stability constants can now be formed according to Eq. (10); these $\log \Delta_{ML}$ values are given in columns 4 and 7 of Table 4. All these values, with the single exception of the values for Mg(DHAP) and Mg(G1P) to which we attribute at present no meaning, are zero within the error limits; hence, no significantly increased stability is observed for any of the binary M(DHAP) and M(G1P) complexes. This result also holds for the ternary Cu(Arm)(DHAP) and Cu(Arm)(G1P) complexes, where Arm = Bpy or Phen (data not listed) [61].

From the above observations it follows that the intramolecular equilibrium (13) lies clearly on the left side. However, one has to be aware that the $\log \Delta_{ML}$ values listed in Table 4 carry error limits. Under the reasonable assumption that a stability increase of 0.1 log unit would have been recognized with certainty [61], one obtains from Eq. (7) $K_I < 26$ and hence, one has to conclude that the upper limit for the occurrence of closed species according to equilibrium (13) is about 20%. In other words, it cannot be ruled out on the basis of the summarized results that $M(DHAP)_{cl}$ and $M(G1P)_{cl}$ occur in aqueous solution in 'traces', e.g. with Mg^{2+}.

4.2. A decreased solvent polarity favors M^{2+} binding of the weakly coordinating oxygen sites!

Since in proteins [62] or in active-site cavities of enzymes [63,64] the so-called 'effective' or 'equivalent solution' dielectric constants are reduced compared to the situation in bulk water, namely, e.g. from about 80 to 35 [63], considerations for a lower solvent polarity are appropriate. The latter mentioned value of 35 is close to the one of water containing 50% (v/v) 1,4-dioxane [65], and therefore, one may attempt to simulate the situation in an active-site cavity by applying water/1,4-dioxane mixtures. In fact, with the last mentioned reasoning of Section 4.1 in mind and by considering that increasing amounts of 1,4-dioxane in an aqueous solution should render solvation of metal ions more difficult, the participation of the oxygen at C2 in complex formation of $DHAP^{2-}$ and $G1P^{2-}$ should become facilitated.

Application of $\log K^{M}_{ML}$ versus pK^{H}_{HL} plots for simple phosphate monoesters also leads to straight lines for water/1,4-dioxane solutions [52–54]; such reference lines are shown in Fig. 4 together with the data pairs for the Cu^{2+} complexes of $DHAP^{2-}$ and $G1P^{2-}$ [61]. It is evident that the overall stability of the Cu^{2+} complexes increases drastically with increasing amounts of 1,4-dioxane, i.e. with a decreasing solvent polarity. More important, however, is the observation that the solid points due to the data pairs for the Cu(DHAP) and Cu(G1P) complexes are more and more above their reference lines. Since the vertical distances between these points and their reference lines correspond to $\log \Delta_{ML}$ as defined by Eq. (10), it is evident that the stability increases for the Cu(DHAP) and Cu(G1P) complexes with increasing amounts of 1,4-dioxane.

Application of the straight-line equations in Table 1 and of the acidity constants of $H(DHAP)^{-}$ and $H(G1P)^{-}$ allows an exact quantification of the stability

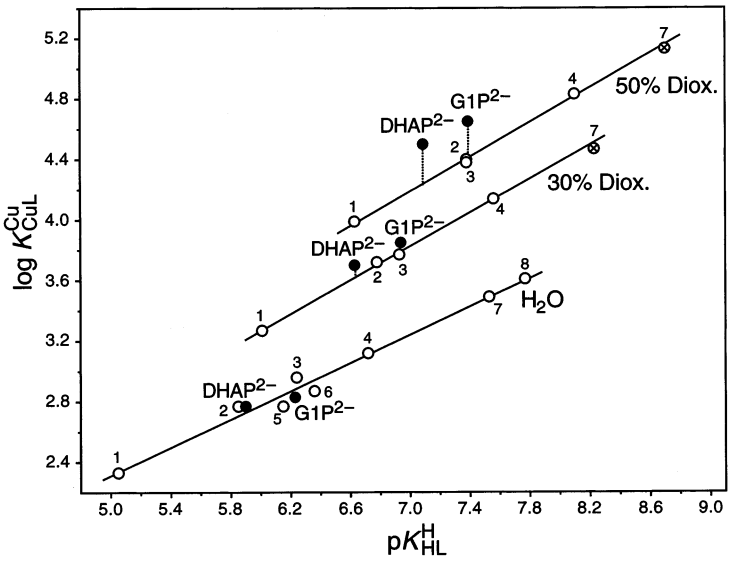

Fig. 4. Evidence for an enhanced stability of the Cu(DHAP) and Cu(G1P) complexes (●) in 1,4-dioxane-water mixtures as solvents based on the relationship between log K^{Cu}_{CuL} and pK^{H}_{HL} for the Cu^{2+} 1:1 complexes of 4-nitrophenyl phosphate (1), phenyl phosphate (2), D-ribose 5-monophosphate (3), *n*-butyl phosphate (4), uridine 5′-monophosphate (5), thymidine 5′-monophosphate (6), methanephosphonate (7), and ethanephosphonate (8) in water and in water containing 30 or 50% (v/v) 1,4-dioxane. The least-squares lines are drawn in each case through the data shown (○) [49,50]; the equations for these reference lines are given in Table 1 (entries 8, 13, and 15). The data points due to the methanephosphonate system in the mixed solvents (⊗) (see Ref. [52]) are shown to prove that simple phosphonates fit within the experimental error limits on the reference lines established with phosphate monoester systems (for details see Ref. [53]). The data pairs for the points due to the Cu^{2+} 1:1 complexes formed with $DHAP^{2-}$ and $G1P^{2-}$ (●) in the three mentioned solvents are taken from Table 3 in Ref. [61] (see also Table 5 in Section 4.2). The vertical broken lines emphasize the stability differences to the corresponding reference lines; these differences are equal to log $\Delta_{Cu(DHAP)}$ and log $\Delta_{Cu(G1P)}$ (Eq. (10)), the values of which are listed in column 7 of Table 5. All of the plotted equilibrium constants refer to 25°C and $I = 0.1$ M ($NaNO_3$).

increases, log Δ_{ML}. These results are summarized in Table 5 together with some pertinent information about the solvents employed. The degree of formation of the chelated isomers of Cu(DHAP) and Cu(G1P) is with about 45% in 50% (v/v) water–dioxane mixtures quite pronounced and therefore, under these conditions equilibrium (13) is important.

4.3. Some general comments also referring to glyceraldehyde 3-phosphate (GAP^{2-})

The stability of the complexes formed between divalent metal ions and $DHAP^{2-}$ or $G1P^{2-}$ (Fig. 1(B)) is governed by the metal ion affinity of the phosphate group. This conclusion is valid for aqueous solution as well as for the mixed solvents. However, in the latter, due to the reduced solvent polarity the carbonyl group of $DHAP^{2-}$ and the hydroxy group of $G1P^{2-}$ can also participate in complex

Table 5
Negative logarithms of the acidity constants (Eq. (9)) of $H(DHAP)^-$ and $H(G1P)^-$, and logarithms of the stability constants of the corresponding Cu(DHAP) and Cu(G1P) complexes (Eqs. (3)–(5)) as determined by potentiometric pH titrations (Exp.) in dependence on the amount of 1,4-dioxane added to water and on the resulting dielectric constant[a]. The stability constants for a pure Cu^{2+}–phosphate residue coordination, i.e. for ML_{op} (Eq. (8)), were calculated (Calc.) with the listed acidity constants and the straight-line equations given in Table 1; the resulting stability differences, log Δ_{CuL}, are defined by Eq. (10). The extent of chelate formation according to equilibrium (13) in the Cu(DHAP) and Cu(G1P) complexes is quantified by the dimensionless equilibrium constant K_I (Eqs. (2) and (7)) and the percentage of the closed isomer, CuL_{cl} (25°C; $I = 0.1$ M, $NaNO_3$)[b]

%(v/v) Dioxane	Mole fraction dioxane	ε[c]	pK^H_{HL}	log K^{Cu}_{CuL}		log Δ_{CuL}	K_I	%CuL_{cl}
				Exp.	Calc.			
$L^{2-} = DHAP^{2-}$								
0	0	78.5	5.90 ± 0.01	2.77 ± 0.02	2.73 ± 0.06	0.04 ± 0.06	0.10 ± 0.16	9 ± 13
30	0.083	52.7	6.63 ± 0.01	3.70 ± 0.02	3.62 ± 0.03	0.08 ± 0.04	0.20 ± 0.10	17 ± 7
50	0.175	35.2	7.09 ± 0.01	4.50 ± 0.01	4.24 ± 0.03	0.26 ± 0.03	0.82 ± 0.13	45 ± 4
$L^{2-} = G1P^{2-}$								
0	0	78.5	6.23 ± 0.01	2.83 ± 0.05	2.88 ± 0.06	-0.05 ± 0.08	0 (<0.08)	0 (<7)
30	0.083	52.7	6.94 ± 0.01	3.85 ± 0.02	3.79 ± 0.03	0.06 ± 0.04	0.15 ± 0.10	13 ± 7
50	0.175	35.2	7.39 ± 0.03	4.65 ± 0.02	4.41 ± 0.03	0.24 ± 0.04	0.74 ± 0.14	42 ± 5

[a] The values in columns 4 and 5 are taken from Table 3 in Ref. [61]. The values listed in columns 6–9 are revised compared to those given in Ref. [61].
[b] For the error limits see footnote 'd' of Table 2.
[c] The dielectric constants for the dioxane–water mixtures are interpolated from the data given in Ref. [65].

formation which gives rise to seven-membered chelates (Eq. (13)) as shown for Cu(DHAP) and Cu(G1P). It is safe to assume that this 'recognition' of the weakly binding O atoms will also hold for other metal ions under conditions of a reduced solvent polarity and that it is therefore of relevance for biological systems. Indeed, it has been suggested that in the active site of class II fructose 1,6-bisphosphate aldolase the coordination of the intrinsic Zn^{2+} to the oxygen atom of the carbonyl group leads to a polarization of this group which then facilitates proton abstraction from the neighboring CH_2 and thus, carbon-carbon bond formation [66] (see also Section 1).

Another point to be made in the present context is that it may be surmised [61] that glyceraldehyde 3-phosphate (GAP^{2-}: HC(O)–CH(OH)–$CH_2OPO_3^{2-}$), which co-exists to about 4% in equilibrium with its keto form $DHAP^{2-}$ [67], shows in M(GAP) complexes to a first approximation the stabilities and properties of the corresponding M(G1P) species because the structural unit, –CH(OH)–$CH_2OPO_3^{2-}$, which is responsible for the coordinating properties, is identical in both ligands. The above assumption is confirmed by the similarity of an apparent pK_a of 6.3 ($I = 0.1$ M; 30°C) for $H(GAP)^-$, as determined by kinetic experiments with triosephosphate isomerase [68], with the value of Table 4 (see footnote 'b'), i.e. $pK^H_{H(GAP)} \simeq pK^H_{H(G1P)} = 6.23$ ($I = 0.1$ M, $NaNO_3$; 25°C). It may be mentioned here that the ketotriose and the aldotriose, i.e. DHAP and GAP, are rapidly interconverted into each other by triosephosphate isomerase [67,69]. The preceding conclusions regarding the metal ion and also proton affinities of GAP^{2-} are important because the properties of this ligand may hardly be studied directly due to its instability [70] in, particularly alkaline, aqueous solution.

5. Isomeric equilibria of complexes formed with acetyl phosphate (AcP^{2-}) and its analogue, acetonylphosphonate (AnP^{2-})

The mixed anhydride of acetic acid and phosphoric acid, acetyl phosphate (AcP^{2-}; Fig. 1(C)), is very sensitive to hydrolysis. Consequently, commercially available AcP always contains phosphate as an impurity; the content of which needs to be determined and monitored during the experiments. In the study discussed below [71], this precondition was fulfilled and the stability of the corresponding M(HPO_4) complexes [72] were considered in the evaluations. Such difficulties do not exist, of course, with the structurally closely related acetonylphosphonate (AnP^{2-}; Fig. 1(C)), which is hydrolysis-stable.

The primary metal ion-binding site in AcP^{2-} and AnP^{2-} is certainly the $-PO_3^{2-}$ group (Fig. 1(C)). However, considering the results summarized in Section 4.2 regarding the participation of the carbonyl oxygen of $DHAP^{2-}$ in the formation of a seven-membered chelate and considering further that the carbonyl oxygen in the acetyl and acetonyl residues of AcP^{2-} and AnP^{2-}, respectively, is located such that six-membered chelates may be formed, the occurrence of an intramolecular equilibrium between an isomer with a sole phosph(on)ate coordination, ML_{op}, and the

chelated species, ML_{cl}, seems quite likely. Hence, equilibrium (14), where X = O (AcP^{2-}) or CH_2 (AnP^{2-}), needs to be considered:

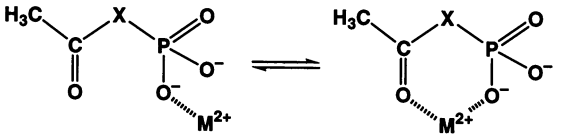

(14)

5.1. Metal ion–carbonyl oxygen recognition in aqueous solution in complexes of AcP^{2-} and AnP^{2-}

From the relationship shown in Fig. 5 between $\log K^{M}_{ML}$ and pK^{H}_{HL} for simple phosph(on)ate complexes of Ba^{2+}, Co^{2+}, and Cu^{2+} and also the inserted data for the corresponding AcP^{2-} systems, it is evident that all the M(AcP) complexes are

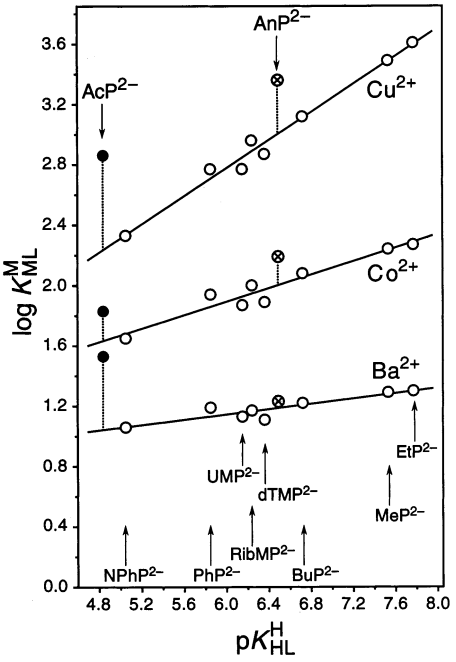

Fig. 5. Evidence for an enhanced stability of the M(AcP) (●) complexes with Ba^{2+}, Co^{2+}, and Cu^{2+} and of some M(AnP) (⊗) complexes based on the relationship between $\log K^{M}_{ML}$ and pK^{H}_{HL} for the 1:1 complexes of Ba^{2+}, Co^{2+}, and Cu^{2+} with the eight simple phosphate monoester or phosphonate ligands listed in the legend of Fig. 2 (○); the equations for the corresponding least-squares reference lines are given in Table 1 (entries 4, 6, and 8). The vertical broken lines emphasize the stability differences of the M(AcP) (●) and M(AnP) (⊗) complexes to the corresponding reference lines; these differences are equal to $\log \Delta_{M(AcP)}$ and $\log \Delta_{M(AnP)}$ (Eq. (10)), the values of which are listed in column 5 of Table 6. The equilibrium constants for the data points due to the AcP and AnP systems are taken from Tables 1 and 2 of Ref. [71] (see also Table 6 in Section 5.1). All plotted equilibrium constant values refer to aqueous solutions at 25°C and $I = 0.1$ M ($NaNO_3$).

considerably more stable than is expected on the basis of the basicity of the AcP^{2-}-phosphate group. Consequently, one has to conclude that equilibrium (14) operates. The Co(AnP) and Cu(AnP) complexes also have an increased stability whereas the data point for the Ba(AnP) complex fits on its reference line (Fig. 5) indicating that in this case the complex with a sole phosphonate-coordination is the crucial one.

Of course, the vertical distances indicated by broken lines in Fig. 5 are identical with the stability differences, $\log \Delta_{ML}$, defined by Eq. (10). Application of the straight-line equations of Table 1 and of the pK^{H}_{HL} values for $H(AcP)^{-}$ and $H(AnP)^{-}$ [71] allows an exact determination of these stability differences; they are listed in column 5 of Table 6; the two columns at the left and next to it provide the stability constants the differences are based on. The results, which quantify the position of equilibrium (14), were obtained with Eqs. (7) and (11); they are given in the two final columns to the right.

Table 6
Comparison of the measured stability constants, K^{M}_{ML} (Eqs. (3)–(5))[a], of the M(AcP) and M(AnP) complexes with the calculated stability constants, $K^{M}_{ML_{op}}$ (Eq. (8))[b], for the isomers with a sole phosph(on)ate coordination of M^{2+}, and extent of the intramolecular chelate formation according to equilibrium (14) in the M(AcP) and M(AnP) complexes as defined by K_I (Eqs. (2) and (7)) and % ML_{cl} (Eq. (11)) for aqueous solutions at 25°C and $I = 0.1$ M ($NaNO_3$)[c]

No.	M^{2+}	$\log K^{M}_{ML}$	$\log K^{M}_{ML_{op}}$ [b]	$\log \Delta_{ML}$	K_I	% ML_{cl}
$L^{2-} = AcP^{2-}$						
1	Mg^{2+}	1.51 ± 0.02	1.28 ± 0.03	0.23 ± 0.04	0.70 ± 0.14	41 ± 5
2	Ca^{2+}	1.55 ± 0.04	1.27 ± 0.05	0.28 ± 0.06	0.91 ± 0.28	48 ± 8
3	Sr^{2+}	1.47 ± 0.02	1.13 ± 0.04	0.34 ± 0.04	1.19 ± 0.23	54 ± 5
4	Ba^{2+}	1.53 ± 0.03	1.04 ± 0.04	0.49 ± 0.05	2.09 ± 0.36	68 ± 4
5	Mn^{2+}	1.95 ± 0.03	1.83 ± 0.05	0.12 ± 0.06	0.32 ± 0.18	24 ± 10
6	Co^{2+}	1.83 ± 0.05	1.63 ± 0.06	0.20 ± 0.08	0.58 ± 0.29	37 ± 11
7	Ni^{2+}	1.75 ± 0.04	1.61 ± 0.05	0.14 ± 0.06	0.38 ± 0.20	28 ± 11
8	Cu^{2+}	2.86 ± 0.05	2.24 ± 0.06	0.62 ± 0.08	3.17 ± 0.75	76 ± 4
9	Zn^{2+}	2.04 ± 0.03	1.65 ± 0.06	0.39 ± 0.07	1.45 ± 0.38	59 ± 6
10	Cd^{2+}	2.18 ± 0.04	1.99 ± 0.05	0.19 ± 0.06	0.55 ± 0.23	35 ± 10
$L^{2-} = AnP^{2-}$						
11	Mg^{2+}	1.73 ± 0.02	1.62 ± 0.03	0.11 ± 0.04	0.29 ± 0.11	22 ± 6
12	Ca^{2+}	1.55 ± 0.01	1.49 ± 0.05	0.06 ± 0.05	0.15 ± 0.13	13 ± 10
13	Sr^{2+}	1.31 ± 0.05	1.26 ± 0.04	0.05 ± 0.06	0.12 ± 0.17	11 ± 13
14	Ba^{2+}	1.23 ± 0.04	1.19 ± 0.04	0.04 ± 0.06	0.10 ± 0.14	9 ± 12
15	Mn^{2+}	2.36 ± 0.02	2.23 ± 0.05	0.13 ± 0.05	0.35 ± 0.17	26 ± 9
16	Co^{2+}	2.19 ± 0.02	2.00 ± 0.06	0.19 ± 0.06	0.55 ± 0.23	35 ± 9
17	Ni^{2+}	2.14 ± 0.02	2.01 ± 0.05	0.13 ± 0.05	0.35 ± 0.17	26 ± 9
18	Cu^{2+}	3.36 ± 0.03	3.00 ± 0.06	0.36 ± 0.07	1.29 ± 0.35	56 ± 7
19	Zn^{2+}	2.47 ± 0.04	2.22 ± 0.06	0.25 ± 0.07	0.78 ± 0.30	44 ± 9
20	Cd^{2+}	2.71 ± 0.03	2.53 ± 0.05	0.18 ± 0.06	0.51 ± 0.20	34 ± 9

[a] These and the other values compiled in this table are abstracted from Tables 2 and 3 in Ref. [71].
[b] Calculated with the acidity constants, $pK^{H}_{H(AcP)} = 4.84 \pm 0.02$ and $pK^{H}_{H(AnP)} = 6.49 \pm 0.02$ [71], and the straight-line equations listed in Table 1.
[c] For the error limits see footnote 'd' of Table 2.

Comparisons of the results in Table 6 show that the formation degrees of chelates formed between Mn^{2+}, Co^{2+}, Ni^{2+}, or Cd^{2+} and AcP^{2-} or AnP^{2-} are identical within the error limits for a given M^{2+} (entries 5–7, 10, and 15–17, 20). In contrast, the M(AcP) complexes of the alkaline earth ions and of Cu^{2+} or Zn^{2+} have larger chelate formation degrees. Maybe the reason is, especially in the case of Cu^{2+} (entries 8, 18) and Zn^{2+} (entries 9, 19) which usually do not have a regular octahedral coordination sphere [73], the smaller angle around the 'anhydride' O in AcP^{2-} (assumed to be close to 104° as in H_2O) compared with the C–(CH_2)–P angle in AnP^{2-} (assumed to be close to 109° as in CH_4). Theoretical calculations [74] also indicate that the $CH_3C(O)$–O bond, that is the one to the 'anhydride' O, has some double bond contribution which is meaningful for a preorientation of the ligand toward complex formation.

Most intriguing, however, is the situation of the alkaline earth ion complexes. Those with AnP^{2-} (Table 6, entries 11–14) show the usual properties, that is, the complex stability decreases with increasing ionic radii. In contrast to this the complexes with AcP^{2-} show not only a relatively high formation degree of the chelates but also a surprising order for the stability increase $\log \Delta_{M(AcP)}$, that is, $Mg^{2+} < Ca^{2+} < Sr^{2+} < Ba^{2+}$ (Table 6, column 5, entries 1–4). This order parallels the ionic radii and therefore, it can not be explained by the usual argument; however, the hydrated radii [75] show the reverse order, that is, Ba^{2+} has the smallest and Mg^{2+} the largest one. Consequently, this indicates that complex formation occurs, at least to some extent, in an outersphere fashion. If this interpretation is correct then hydrogen bonding is important and here AcP^{2-} is clearly to be favored over AnP^{2-} because the 'anhydride' O may participate in it whereas the methylene group is unable to do so. Into this same argument also fits the observation that the methylene group will hinder solvation of the complex whereas the 'anhydride' oxygen will favor it.

However, in both complex series, M(AcP) and M(AnP), chelate formation plays a significant role and this is even somewhat more pronounced in the M(AcP) species (Table 6, column 7). In this context recent ab initio molecular orbital calculations [74] carried out for AcP^{2-} at the STO-3G level in the gas phase are of interest. They provided on average a net atomic charge of -0.697 for each of the three terminal oxygen atoms of the $-PO_3^{2-}$ group and a charge of -0.473 for the carbonyl oxygen of the acetyl residue. This relatively high charge density on the carbonyl oxygen makes this atom evidently quite suitable for an interaction with metal ions, and in fact, this is what the results of Table 6 prove (for further details see Ref. [71]). Thus, equilibrium (14) is of relevance for all of the M(AcP) and for most of the M(AnP) complexes; in other words, all biologically important metal ions 'recognize' the carbonyl oxygen of AcP^{2-} and AnP^{2-} in aqueous solution, if they are already phosph(on)ate-coordinated.

5.2. How is the situation in mixed ligand complexes and what is the effect of a reduced solvent polarity on carbonyl-oxygen binding?

Since in an enzymatic reaction complex formation at the active site usually involves several species [2], the formation of higher order complexes is of interest.

Table 7
Effect of mixed ligand complex formation on the stability difference log $\Delta_{M(AcP)}$ as defined by Eq. (10), and on the extent of chelate formation (Eq. (14)) in the ternary Cu(Bpy)(AcP) and Cu(Phen)(AcP) complexes as quantified by the dimensionless equilibrium constant K_I (Eqs. (2) and (7)) and the percentage of the closed isomer, $M(AcP)_{cl}$ (Eq. (11)), for aqueous solutions at 25°C and $I = 0.1$ M ($NaNO_3$)[a]

M^{2+}	log $\Delta_{M(AcP)}$	K_I	% $M(AcP)_{cl}$
Cu^{2+}	0.62 ± 0.08	3.17 ± 0.75	76 ± 4
$Cu(Bpy)^{2+}$	0.61 ± 0.11	3.07 ± 1.00	75 ± 6
$Cu(Phen)^{2+}$	0.62 ± 0.08	3.17 ± 0.75	76 ± 4

[a] Line 1 is from Table 6; the other data are abstracted from Table 3 of Ref. [76] where also the stability constants, $K^{M}_{M(AcP)}$ (Eqs. (3)–(5)), are given. For the error limits see footnote 'd' of Table 2.

In other words: Will the carbonyl oxygen of AcP^{2-} and AnP^{2-} still participate in complex formation if part of the coordination sphere of the metal ion involved is already occupied by another ligand? This question was addressed by using $Cu(Bpy)^{2+}$ and $Cu(Phen)^{2+}$ for the formation of mixed ligand complexes with AcP^{2-} and AnP^{2-} [76]. The pertinent results for the ternary complexes with AcP^{2-} are summarized in Table 7.

The answer to the above question is surprisingly simple: The formation degree of the chelated isomer in equilibrium (14) is close to 75% and within the error limits identical for Cu(AcP), Cu(Bpy)(AcP) and Cu(Phen)(AcP) (Table 7). Furthermore, there is no reason to assume that this will be different with Zn^{2+} or other metal ions of biological relevance. Hence, we may conclude that as long as a partially saturated coordination sphere of a metal ion has still easily accessible further sites, the carbonyl oxygen can be bound.

Considering the reduced 'effective' or 'equivalent solution' dielectric-constant situation in active-site cavities of enzymes as discussed in the first paragraph of Section 4.2 and knowing that charge-type interactions in the M(AcP) and M(AnP) complexes are clearly important as discussed above in Section 5.1, the effect of a decreasing solvent polarity on the stability of the complexes needs to be evaluated. Corresponding studies in water containing 1,4-dioxane exist for the complexes formed between AnP^{2-} and Cu^{2+} [71] or $Cu(Bpy)^{2+}$ [76].

The necessary reference lines for a quantitative evaluation are available (Table 1); in fact, the situation for the AnP systems is comparable to that seen in Fig. 4 for the $DHAP^{2-}$ and $G1P^{2-}$ complexes, but the stability enhancements as expressed by log Δ_{ML} (Eq. (10)) are more pronounced [71,76]. The results summarized in Table 8 demonstrate that the stability differences log $\Delta_{M(AnP)}$ clearly increase with increasing 1,4-dioxane concentration in the solvent, indicating that equilibrium (14) is progressively shifted toward its right-hand side. Indeed, entries 1–3 and 4–6 confirm for Cu(AnP) and Cu(Bpy)(AnP), respectively, that the degree of formation of the chelated isomer increases from about 55% in water to close to 80% in water containing 50% dioxane. The binary and ternary systems behave correspondingly as, e.g. a comparison of entries 1 and 4 or 3 and 6 reveals. Hence, a decreasing

Table 8
Effect of a reduced solvent polarity on the stability difference log $\Delta_{M(AnP)}$ as defined by Eq. (10), and on the extent of chelate formation (Eq. (14)) in the binary Cu(AnP) and the ternary Cu(Bpy)(AnP) complexes as quantified by the dimensionless equilibrium constant K_I (Eqs. (2) and (7)) and the percentage of the closed isomer, $M(AnP)_{cl}$ (Eq. (11)), in water and in water containing 30 or 50% (v/v) 1,4-dioxane at 25°C and $I = 0.1$ M ($NaNO_3$)[a]

No.	M^{2+}	% (v/v) dioxane	log $\Delta_{M(AnP)}$	K_I	% $M(AnP)_{cl}$
1	Cu^{2+}	0	0.36 ± 0.07	1.29 ± 0.35	56 ± 7
2	Cu^{2+}	30	0.51 ± 0.04	2.24 ± 0.32	69 ± 3
3	Cu^{2+}	50	0.70 ± 0.04	4.01 ± 0.42	80 ± 2
4	$Cu(Bpy)^{2+}$	0	0.37 ± 0.08	1.34 ± 0.41	57 ± 7
5	$Cu(Bpy)^{2+}$	30	0.50 ± 0.04	2.16 ± 0.33	68 ± 3
6	$Cu(Bpy)^{2+}$	50	0.62 ± 0.07	3.17 ± 0.70	76 ± 4

[a] Entry 1 is from Table 6; the other data are abstracted from Table 5 in Ref. [71] and Table 3 in Ref. [76] where also the stability constants, $K^{M}_{M(AnP)}$ (Eqs. (3)–(5)), are given. For the error limits see footnote 'd' of Table 2.

solvent polarity favors metal ion binding of the carbonyl oxygen; a result that confirms the observations made with $DHAP^{2-}$ (Section 4.2; Table 5).

6. The 'peculiar' properties of metal ion complexes formed with flavin mononucleotide (FMN^{2-})

The ribityl part of FMN^{2-}, which encompasses the carbons C3′, C4′, and C5′, corresponds in its structure to glycerol 1-phosphate ($G1P^{2-}$; cf. Fig. 1(D)). The results seen in Fig. 6 for the FMN^{2-} complexes of Mg^{2+}, Zn^{2+}, and Cu^{2+} [77] may therefore appear as somewhat surprising, and indeed they are as we shall see below. In accord with the results discussed in Section 4.1, the data points for the corresponding $G1P^{2-}$ complexes fit within their error limits on the reference lines whereas those for FMN^{2-} are clearly above these lines indicating an increased stability of the M(FMN) complexes. A careful evaluation of the results [77] which are summarized in Table 9 confirms that all the M(FMN) complexes studied are somewhat more stable than is expected on the basis of the basicity of the FMN^{2-}-phosphate residue. The stability increase, as defined by Eq. (10), amounts on average for the 10 systems considered to $\log \Delta_{M(FMN)/av} = 0.16 \pm 0.04$ (3σ) [77]. In an earlier study [78] a similar stability enhancement has been observed for Ni(FMN), i.e. $\log \Delta_{Ni(FMN)} = 0.17$ [77,78].

There is no doubt, the mentioned stability increase (see Table 9, column 4) is small, yet it is certainly real as follows from the two independent studies [77,78]. But where does the increased stability of the M(FMN) complexes originate? In the earlier kinetic study [78] it was suggested that phosphate-bound Ni^{2+} interacts simultaneously with the isoalloxazine moiety. Is this suggestion supported by the results of Table 9? It is remarkable that the stability increase observed for the various M(FMN) complexes is independent of the metal ion; it is always between

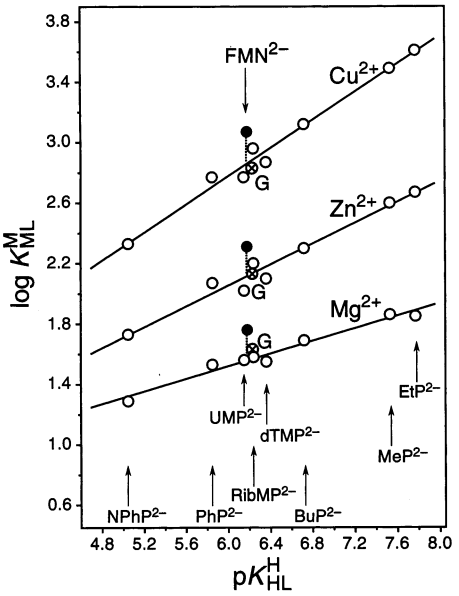

Fig. 6. Evidence for an enhanced stability of several M(FMN) complexes (●), based on the relationship between log K^{M}_{ML} and pK^{H}_{HL} for the 1:1 complexes of Mg^{2+}, Zn^{2+}, and Cu^{2+} with the eight simple phosphate monoester or phosphonate ligands listed in the legend of Fig. 2 (○); the equations for the corresponding least-squares reference lines are given in Table 1 (entries 1, 9, and 8). The vertical broken lines emphasize the stability differences of the M(FMN) complexes (●) to the corresponding reference lines; these differences are equal to log $\Delta_{M(FMN)}$ as defined in Section 2 by Eq. (10), the values of which are listed in column 4 of Table 9. The data points due to the M(G1P) complexes (G; ⊗) are given for comparison; all of them fall within the error limits on the reference lines (see also column 7 of Table 9). The equilibrium constants for the data points due to the FMN and G1P systems are taken from Tables 1 and 2 of Ref. [77] (see also Table 4 in Section 4.1). All plotted equilibrium constant values refer to aqueous solutions at 25°C and $I = 0.1$ M ($NaNO_3$).

log $\Delta_{M(FMN)} = 0.1$ and 0.2 (see column 4 of Table 9). Indeed, the mentioned average stability increase log $\Delta_{M(FMN)/av} = 0.16 \pm 0.04$ (3σ) is within its error limits *identical* with the individual values determined for the various M(FMN) complexes. This observation allows the conclusion that, if the stability increase is indeed due to a specific interaction, the binding site with which the phosphate-coordinated metal ion is interacting *cannot* be a nitrogen atom; i.e. N1 and N5 of the isoalloxazine residue are ruled out because the intensity of a nitrogen–metal ion interaction, giving rise to the formation of a macrochelate, should significantly depend on the kind of metal ion involved [48,79]. In other words, the equality of the log $\Delta_{M(FMN)}$ values for the various M(FMN) complexes indicates that, if the interaction is specific, it might rather occur with an oxygen site.

With the above reasoning in mind one is tempted to consider the possibility of chelate formation involving the ribit-hydroxy group at C4′. However, together with the $-PO_3^{2-}$ group this would give rise to the intramolecular equilibrium (13) (already considered in Section 4), but this explanation does not hold because the M(G1P) complexes show no increased stability (Table 9, column 7) despite the identity of the crucial ligand part of FMN^{2-} and $G1P^{2-}$ as is seen in Fig. 1(D).

At this point it has to be concluded that the source of the increased stability must be connected with the isoalloxazine residue of FMN^{2-}. This concurs with the mentioned kinetic study [78] in which next to a fast Ni^{2+}–phosphate interaction a *slow* relaxation effect was observed at about 500 nm, i.e. in this part of the visible spectrum where FMN exhibits a strong absorption.

Taking further into account the above mentioned conclusion that in the case of a specific interaction this should be attributed to an oxygen site, we considered space-filling molecular models: These suggest that the carbonyl oxygen at C2 of the isoalloxazine residue is accessible more easily for the formation of a macrochelate than the one at C4. This then would lead to a concentration-independent equilibrium between an 'open' isomer, $M(FMN)_{op}$, in which the metal ion is only phosphate-coordinated, and a macrochelated or 'closed' species, $M(FMN)_{cl}$, in which the phosphate-bound metal ion also interacts with the carbonyl oxygen of C2. Application of $\log \Delta_{M(FMN)/av} = 0.16 \pm 0.04$ to Eq. (7) results in $K_I = 0.45 \pm 0.13$ (3σ) and a degree of formation of $31 \pm 6\%$ (3σ) for the macrochelated isomer. It is amazing to note that this average degree of formation is within error limits identical with the corresponding degree of formation of 38 ($\pm$ 10)% for $Ni(FMN)_{cl}$, which follows [77] from *kinetic* results [78]; moreover, the already mentioned corresponding stability data for $\log \Delta_{Ni(FMN)}$ (0.17) yield [77] 32% for $Ni(FMN)_{cl}$.

Table 9
Logarithms of the stability constants of M(FMN) complexes (Eqs. (3)–(5)) as determined by potentiometric pH titrations (Exp.) in aqueous solution at 25°C and $I = 0.1$ M ($NaNO_3$), together with the calculated stability constants for a sole metal ion–phosphate residue coordination (Calc.), i.e. for $M(FMN)_{op}$ (Eq. (8)); these latter values, given for comparison, are based on the straight-line equations (quantifying the relationship between complex stability and phosphate-group basicity as) listed in Table 1 and $pK^{H}_{H(FMN)} = 6.18 \pm 0.01$ [77] for the deprotonation of $H(FMN)^-$. The resulting stability differences according to Eq. (10) are listed in the fourth column under $\log \Delta_{M(FMN)}$. To facilitate the direct comparisons between the M(FMN) and the related M(G1P) data the values of the latter systems are taken from Table 4 and given again below on the right-hand side[a,b]

M^{2+}	$\log K^{M}_{M(FMN)}$		$\log \Delta_{M(FMN)}$	$\log K^{M}_{M(G1P)}$		$\log \Delta_{M(G1P)}$
	Exp.	Calc.		Exp.	Calc.	
Mg^{2+}	1.76 ± 0.05	1.56 ± 0.03	0.20 ± 0.06	1.63 ± 0.03	1.57 ± 0.03	0.06 ± 0.04
Ca^{2+}	1.57 ± 0.03	1.45 ± 0.05	0.12 ± 0.06	1.43 ± 0.02	1.45 ± 0.05	-0.02 ± 0.05
Sr^{2+}	1.35 ± 0.03	1.24 ± 0.04	0.11 ± 0.05	1.23 ± 0.03	1.24 ± 0.04	-0.01 ± 0.05
Ba^{2+}	1.37 ± 0.05	1.16 ± 0.04	0.21 ± 0.06	1.18 ± 0.03	1.16 ± 0.04	0.02 ± 0.05
Mn^{2+}	2.28 ± 0.05	2.15 ± 0.05	0.13 ± 0.07	2.21 ± 0.04	2.17 ± 0.05	0.04 ± 0.06
Co^{2+}	2.08 ± 0.05	1.93 ± 0.06	0.15 ± 0.08	1.93 ± 0.02	1.94 ± 0.06	-0.01 ± 0.06
Ni^{2+}	2.05 ± 0.07	1.94 ± 0.05	0.11 ± 0.09	1.90 ± 0.04	1.95 ± 0.05	-0.05 ± 0.06
Cu^{2+}	3.07 ± 0.06	2.86 ± 0.06	0.21 ± 0.08	2.83 ± 0.05	2.88 ± 0.06	-0.05 ± 0.08
Zn^{2+}	2.31 ± 0.06	2.12 ± 0.06	0.19 ± 0.08	2.13 ± 0.04	2.13 ± 0.06	0.00 ± 0.07
Cd^{2+}	2.60 ± 0.04	2.43 ± 0.05	0.17 ± 0.06	2.43 ± 0.03	2.45 ± 0.05	-0.02 ± 0.06

[a] The core of this table is reprinted from Table 2 of Ref. [77] by permission of Elsevier Science S.A., Lausanne, Switzerland.

[b] For the error limits see footnote 'd' of Table 2.

Though the above mentioned suggestion that the increased stability of the M(FMN) complexes is due to a carbonyl oxygen interaction of the isoalloxazine residue with the already phosphate-bound metal ion seems to be quite appealing, we are rather reluctant [77] to propose such an interaction because so far carbonyl oxygen atoms never appeared as attractive binding sites in the formation of macrochelates in all our studies involving nucleotide–metal ion complexes [11,12,50,79,80], despite the fact that such carbonyl groups are quite common in nucleobase residues.

In addition to the caveat mentioned above, one should also point out that even for a weak interaction with an oxygen site, e.g. an ether or carbonyl oxygen atom, some systematic dependence on the kind of metal ion involved usually occurs, as is seen from the results summarized in Tables 3 and 6. Hence, we are faced with the fact that the 7,8-dimethylisoalloxazine residue is in all likelihood responsible for the observed stability increase of the M(FMN) complexes, but that there is no site available to which a metal ion interaction may be convincingly attributed. Therefore, we have been asking ourselves [77]: does the flavin residue simply reduce the 'effective' dielectric constant in the vicinity of the metal ion? Such a reduction of the 'effective' dielectric constant would strengthen the ionic $-PO_3^{2-}-M^{2+}$ interaction [63] and possibly even favor the formation of the seven-membered chelate according to equilibrium (13) or the interaction with a carbonyl oxygen in accord with the results summarized in Section 4.2.

If the presented assumption is correct, it would mean that there are M(FMN) species in which the FMN^{2-} ligand is stretched out with the isoalloxazine residue relatively far away from the metal ion, and others in which the hydrophobic flavin residue is close to the metal ion exerting its influence on the 'effective' dielectric constant. Evidently, this would also alter somewhat the optical absorption properties of the flavin residue. It may be added that among the 'folded' M(FMN) species there is one in which the CH units of the ribityl residue are close to the isoalloxazine ring, allowing a hydrophobic interaction as is easily seen from space-filling molecular models. After much consideration we are led to the assumption [77] that the folded species, with their rather unspecific 'interactions', are the source of the described stability increase ($\log \Delta_{M(FMN)/av} = 0.16$; see also Table 9, column 4) of the M(FMN) complexes. Of course, this also means that it is the *sum* of the degrees of formation for *all* these folded species which amounts in total to about 30% (see above).

Whether the given explanation [77] that a reduction of the 'effective' dielectric constant due to the flavin residue close to the metal ion is the cause for the increased complex stability of the M(FMN) species, is proven in the future as correct or not, the experimental fact remains that the 7,8-dimethylisoalloxazine residue increases complex stability by about 0.2 log units beyond that expected for a sole phosphate–metal ion interaction (Table 9).

The stacking properties of the flavin residue of FMN are known to be important for the biological properties of this coenzyme [36,39]. Indeed, the self-association tendency of FMN^{2-} [81] as well as the intramolecular stack formation in suitable mixed ligand complexes are well documented [82]. For example, the stability of the

Cu(Phen)(FMN) complex [82] is enhanced by about 1 log unit due to intramolecular stacks, the formation degree of which amounts to about 90%. This together with the described effects of the isoalloxazine residue on binary M(FMN) complexes demonstrates that FMN^{2-} is a fascinating ligand with unexpected properties due to the interplay between the isoalloxazine and phosphate residues; consequently, in the presence of metal ions both sides should never be considered independently of each other.

7. General conclusions

In Sections 3–5 we have repeatedly seen that weak interactions involving, e.g. ether or carbonyl oxygen atoms can give rise to intramolecular equilibria of metal ion complexes in solution; these results are unequivocal. The conclusion of Section 6, in which we attributed the observed stability increase of the M(FMN) complexes to the hydrophobic influence of the bulky isoalloxazine residue, is less certain. More work needs to be done on the effects that bulky and hydrophobic groups exert on complex stability, though one may add here that it is well known (e.g. [83,84]) that aromatic residues in the solid state are often found in the vicinity of a metal ion and that this also applies to solutions of complexes containing ligands with aromatic [85–87] and/or aliphatic [87–89] residues. The possible influence of such residues on complex stability by a change in the 'effective' dielectric microenvironment was recognized [86,87,89]. In previous studies dealing with intramolecular ligand-ligand interactions in mixed ligand complexes results obtained for aqueous organic solvent mixtures [85,89] also provided hints for the crucial role of a change in the 'effective' dielectric constant close to the metal ion. However, as indicated above, more work is needed in this direction; this is compulsory for a quantification of the effects observed in many active-site cavities of enzymes, where hydrophilic and hydrophobic regions are in interplay with each other.

In this context the results summarized in column 4 of Table 5 warrant mentioning. These data indicate that a shift of a substrate by a few Ångströms at the 'surface' of a protein from a hydrophilic to a hydrophobic region (and vice versa) may drastically alter the acid–base properties of a phosphate group. This then has effects on the stability of the connected complexes (Table 5, column 5; see also Fig. 4). More important, weak interactions as they occur with carbonyl oxygen atoms or hydroxy groups are especially affected (Tables 5 and 8). In these instances a change of the local ('effective') dielectric constant may give rise to an interaction but also to a complete release of a certain site from the coordination sphere of a metal ion. It may be added that such weak interactions are not only facilitated by a phosphate group as primary binding site (as discussed in this review) but that an imidazole residue can do the same job as well [90].

A further point, which warrants emphasis, is that weak interactions between metal ions and oxygen atoms of carbonyl or hydroxy groups (Tables 5 and 8) on the one hand and nitrogen atoms on the other [52,91] may be affected very differently by decreasing solvent polarity. An example for the latter situation [91] is

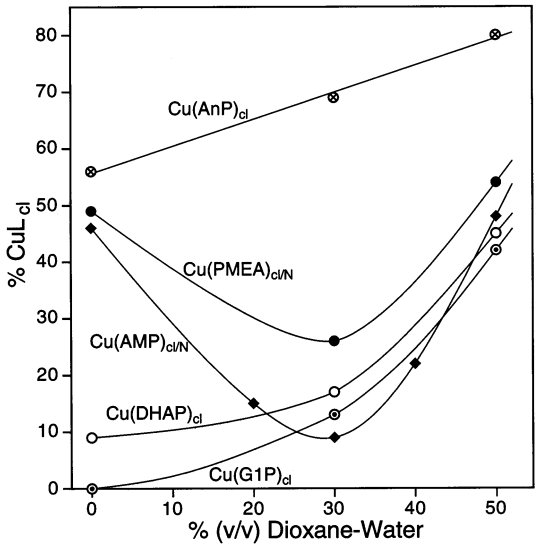

Fig. 7. Formation degree of the chelated isomers, CuL_{cl}, in the Cu(AnP) (cf. Eq. (14), Table 8) as well as the Cu(DHAP) and Cu(G1P) (cf. Eq. (13), Table 5) complex systems as a function of the percentage of 1,4-dioxane added to the aqueous reagent mixtures. For comparison the corresponding dependence is shown for $Cu(AMP)_{cl/N}$, which represents the macrochelate [12,48,79a] involving the phosphate group and N7 of the adenine residue (data from Ref. [91]), as well as for $Cu(PMEA)_{cl/N}$, which represents the $Cu(PMEA)_{cl/O/N3}$ isomer in which Cu^{2+} is initially bound to the phosphonate group and the ether oxygen (see Fig. 3) and then in addition to N3 of the adenine residue forming a seven-membered chelate [22,59] (data from Ref. [52]). All the plotted equilibrium constants refer to 25°C and $I = 0.1$ M ($NaNO_3$).

the formation of macrochelates as it occurs with purine nucleotides, where a phosphate-coordinated metal ion may also interact with N7 of the purine residue [12,48,79]. This point is demonstrated in Fig. 7, where the formation degrees of the six-membered chelate of Cu(AnP) and of the seven-membered chelates of Cu(DHAP) and Cu(G1P) are plotted as a function of the percentage of 1,4-dioxane added to water and where the solvent effect [91] on the formation degree of the macrochelate [48] formed by the phosphate-coordinated Cu^{2+} in its adenosine 5′-monophosphate (AMP^{2-}) complex with N7 of the adenine residue is also shown. A further example for the solvent effect on a weak nitrogen coordination is given by the Cu(PMEA) complex [52] (see Fig. 3), where a seven-membered chelate forms, involving N3 of the purine residue (for details see Ref. [59]). The formation degrees of the chelated $Cu(AMP)_{cl/N}$ and $Cu(PMEA)_{cl/N}$ isomers pass through minima in their dependence on the solvent composition [52,91] whereas the degrees of formation of chelates involving carbonyl or hydroxyl oxygen atoms, i.e. for $Cu(DHAP)_{cl}$, $Cu(G1P)_{cl}$ and $Cu(AnP)_{cl}$, continuously increase. These results provide hints about the subtle ways in which nature may alter the structure of a substrate for a ‘recognition’ reaction.

In enzymatic reactions, where a continuous and rapid turnover of substrate molecules is anticipated and where metal ions are involved, these metal ions need to

be positioned or anchored. This occurs via amino acid residues of the protein, like imidazole or carboxylate groups, which in part occupy the coordination sphere of a metal ion. On the other hand, the other part of the coordination sphere is involved in the actual catalytic process and here weak binding is desirable, since the products must be released after the reaction. To emphasize the relation between the stability enhancement and the change in free energy in dependence on the formation degree of a certain isomeric species Fig. 8 was constructed. The contribution of the closed isomers to the change in free energy for complex formation is given by $\Delta G° = -RT \ln \Delta_{ML}$, i.e. for 25°C it holds that $\Delta G°_{(25°C)} = -5.71 \log \Delta_{ML}$. It can be seen from Fig. 8 that for example a small stability enhancement of $\log \Delta_{ML} = 0.1$ means that already 20% of the closed species is formed, but that this corresponds only to a change in free energy of $\Delta G° = -0.57$ kJ mol^{-1}. When 50% of the complexes exist in the closed form, then $\log \Delta_{ML} = 0.3$ and $\Delta G° = -1.71$ kJ mol^{-1}. Evidently, degrees of formation in this order of the correct structure are enough that a substrate is accepted as such in an enzymatic reaction. On the other hand, when high formation degrees of the closed species are desired, matters become quickly very 'costly'; e.g. degrees of formation of 90 or 99.9% correspond to stability enhancements of 1 or 3 log units and to $\Delta G°$ values of -5.71 or -17.13 kJ mol^{-1}, respectively. Overall, it is clear from Fig. 8 that the presence of a relatively weak binding site in a ligating molecule may have a profound effect on the structure of a complex in solution.

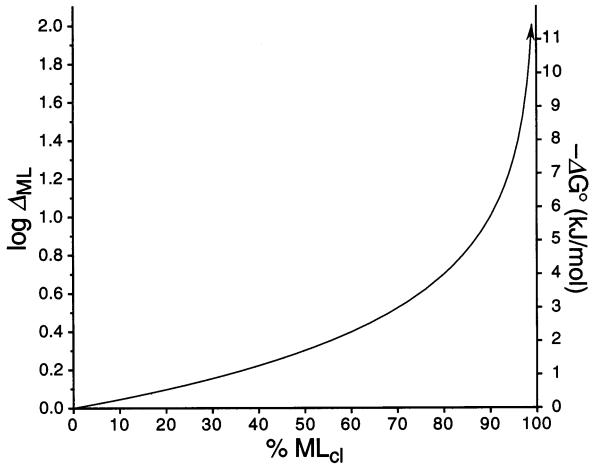

Fig. 8. Relation between the stability enhancement, $\log \Delta_{ML}$ (left-hand ordinate), as defined by Eq. (10) and the formation degree of the closed isomer, ML_{cl}, in equilibrium (1) as defined by Eq. (11). The right-hand ordinate indicates the values in kJ mol^{-1} at 25°C of the contribution of the closed species, ML_{cl}, to the free energy change, $\Delta G°$, for complex formation. The position of the arrow head (at the upper right) defines the point where 99% of a complex exist as the closed isomer and consequently equilibrium (1) is significantly displaced to its right side; at this point $\log \Delta_{ML} = 2.0$ and $\Delta G° = -11.4$ kJ mol^{-1}. (This is a revised version of an earlier similar plot, which was constructed for 20°C [47]).

8. Abbreviations and definitions

AcP^{2-}	acetyl phosphate (Fig. 1(C))
AnP^{2-}	acetonylphosphonate (Fig. 1(C))
Arm	heteroaromatic nitrogen base, e.g. Bpy or Phen
ATP^{4-}	adenosine 5′-triphosphate
Bpy	2,2′-bipyridine
$DHAP^{2-}$	dihydroxyacetone phosphate (Fig. 1(B))
FAD	flavin adenine dinucleotide
$FADH_2$	reduced form of FAD
FMN^{2-}	flavin mononucleotide (= riboflavin 5′-phosphate) (Fig. 1(D))
GAP^{2-}	glyceraldehyde 3-phosphate
$G1P^{2-}$	glycerol 1-phosphate (= α-glycerophosphate; in many biochemistry texts also designated as glycerol 3-phosphate) (Fig. 1(B))
L^{2-}	any phosph(on)ate ligand ($R\text{-}PO_3^{2-}$)
M^{2+}	any divalent metal ion (in a few instances also $Cu(Bpy)^{2+}$ and $Cu(Phen)^{2+}$ are represented by this abbreviation)
NAD^+	nicotinamide adenine dinucleotide
NADH	reduced form of NAD^+
Phen	1,10-phenanthroline
PME^{2-}	dianion of (phosphonomethoxy)ethane (= ethoxymethanephosphonate) (Fig. 1(A))

Species that are given in the text without a charge either do not carry one or represent the species in general (i.e. independent of their degree of protonation); which of the two versions applies is always clear from the context. A few additional definitions are given in Fig. 3 and in the legend to Fig. 2.

Acknowledgements

The competent technical assistance of Ms Rita Baumbusch in the preparation of the manuscript and the support of our research on phosph(on)ate complexes by the Swiss National Science Foundation are gratefully acknowledged.

References

[1] F.H. Westheimer, Science 235 (1987) 1173–1178.
[2] J.J.R. Fraústo da Silva, R.J.P. Williams, The Biological Chemistry of the Elements, Clarendon Press, Oxford, 1991.
[3] H. Sigel, A. Sigel (Eds.), Metal Ions in Biological Systems, vol. 25, Interrelations Among Metal Ions, Enzymes, and Gene Expression, Marcel Dekker, New York and Basel, 1989.
[4] A. Sigel, H. Sigel (Eds.), Metal Ions in Biological Systems, vol. 32, Interactions of Metal Ions with Nucleotides, Nucleic Acids, and Their Constituents, Marcel Dekker, New York, Basel and Hong Kong, 1996.

[5] A. Sigel, H. Sigel (Eds.), Metal Ions in Biological Systems, vol. 33, Probing of Nucleic Acids by Metal Ion Complexes of Small Molecules, Marcel Dekker, New York, Basel and Hong Kong, 1996.
[6] (a) S.A.A. Sajadi, B. Song, F. Gregáň, H. Sigel, Inorg. Chem. 38 (1999) 439–448. (b) E.M. Bianchi, S.A.A. Sajadi, B. Song, H. Sigel, Inorg. Chim. Acta 300–302 (2000) 487–498.
[7] R.M. Smith, A.E. Martell, Y. Chen, Pure Appl. Chem. 63 (1991) 1015–1080.
[8] L.D. Pettit, H.K.J. Powell, IUPAC Stability Constants Database, Version 3.02, Academic Software, Timble, Otley, West Yorkshire, UK, 1998.
[9] R.M. Smith, A.E. Martell, NIST Critically Selected Stability Constants of Metal Complexes, Reference database 46, Version 5.0, US Department of Commerce, National Institute of Standards and Technology, Gaithersburg, MD, USA, 1998.
[10] K. Murray and P.M. May, Joint Expert Speciation System (JESS), Version 5.3b, Joint Venture by the Division of Water Technology, CSIR, Pretoria, South Africa, and the School of Mathematical and Physical Sciences, Murdoch University, Murdoch, Western Australia, 1996.
[11] H. Sigel, Chem. Soc. Rev. 22 (1993) 255–267.
[12] H. Sigel, B. Song, Met. Ions Biol. Syst. 32 (1996) 135–205; cf. Ref. [4].
[13] R.K.O. Sigel, B. Song, H. Sigel, J. Am. Chem. Soc. 119 (1997) 744–755.
[14] R. Kluger, R.W. Loo, V. Mazza, J. Am. Chem. Soc. 119 (1997) 12089–12094.
[15] J.D. Rawn, Biochemistry, Patterson, Burlington, NC, 1989.
[16] D. Voet, J.G. Voet, Biochemistry, 2nd ed., Wiley, New York, 1995.
[17] (a) J.C. Martin (Ed.), Nucleotide Analogues as Antiviral Agents, ACS Symposium Series 401, American Chemical Society, Washington, DC, USA, 1989. (b) M.R. Harnden (Ed.), Approaches to Antiviral Agents, VCH, Weinheim, 1985.
[18] E. De Clercq, Collect. Czech. Chem. Commun. 63 (1998) 449–479 and 480–506.
[19] F. Franek, A. Holý, I. Votruba, T. Eckschlager, Int. J. Oncol. 14 (1999) 745–752.
[20] (a) H. Sigel, Coord. Chem. Rev. 144 (1995) 287–319. (b) H. Sigel, J. Indian Chem. Soc. 74 (1997) 261–271 (P. Ray Award Lecture).
[21] (a) A. Holý, E. De Clercq, I. Votruba, ACS Symp. Ser. 401 (1989) 51–71; cf. Ref. [17a]. (b) D. Villemin, F. Thibault-Starzyk, Synth. Commun. 23 (1993) 1053–1059.
[22] H. Sigel, Pure Appl. Chem. 71 (1999) 1727–1740.
[23] H. Sigel, B. Song, C.A. Blindauer, L.E. Kapinos, F. Gregáň, N. Prónayová, Chem. Commun. (1999) 743–744.
[24] L. Stryer, Biochemistry, 4th ed., Freeman, New York, 1997.
[25] (a) P.V. Racenis, J.L. Lai, A.K. Das, P.C. Mullick, A.K. Hajra, M.L. Greenberg, J. Bacteriol. 174 (1992) 5702–5710. (b) M. Nishihara, T. Yamazaki, T. Oshima, Y. Koga, J. Bacteriol. 181 (1999) 1330–1333.
[26] (a) D.R. Hall, G.A. Leonard, C.D. Reed, C.I. Watt, A. Berry, W.N. Hunter, J. Mol. Biol. 287 (1999) 383–394. (b) S.J. Cooper, G.A. Leonard, S.M. McSweeney, A.W. Thompson, J.H. Naismith, S. Qamar, A. Plater, A. Berry, W.N. Hunter, Structure 4 (1996) 1303–1315.
[27] (a) L.-Å. Idahl, N. Lembert, Biochem. J. 312 (1995) 287–292. (b) V.N. Civelek, J.T. Deeney, N.J. Shalosky, K. Tornheim, R.G. Hansford, M. Prentki, B.E. Corkey, Biochem. J. 318 (1996) 615–621.
[28] For example: (a) T.L. Mayover, C.J. Halkides, R.C. Stewart, Biochemistry 38 (1999) 2259–2271. (b) S.S. Da Re, D. Deville-Bonne, T. Tolstykh, M. Véron, J.B. Stock, FEBS Lett. 457 (1999) 323–326. (c) C.L. Sodré, H.M. Scofano, H. Barrabin, Biochim. Biophys. Acta 1419 (1999) 55–63. (d) T. Tsuda, S. Kaya, T. Yokoyama, Y. Hayashi, K. Taniguchi, J. Biol. Chem. 273 (1998) 24339–24345.
[29] C.G. Head, A. Tardy, L.J. Kenney, J. Mol. Biol. 281 (1998) 857–870.
[30] (a) M.G.N. Hartmanis, Met. Ions Biol. Syst. 30 (1994) 201–215; cf. Ref. [30d]. (b) T. Toraya, Met. Ions Biol. Syst. 30 (1994) 217–254 (see p. 245–247). (c) K.K. Wong, J.W. Kozarich, Met. Ions Biol. Syst. 30 (1994) 279–313 (see p. 281). (d) H. Sigel, A. Sigel (Eds.), Metal Ions in Biological Systems, vol. 30, Metalloenzymes Involving Amino Acid-Residue and Related Radicals, Marcel Dekker, New York, Basel and Hong Kong, 1994.
[31] (a) A.-K. Bock, J. Glasemacher, R. Schmidt, P. Schönheit, J. Bacteriol. 181 (1999) 1861–1867. (b) S. Kumari, R. Tishel, M. Eisenbach, A.J. Wolfe, J. Bacteriol. 177 (1995) 2878–2886.

[32] (a) H. Ishikawa, M. Shiroshima, A. Widjaja, H. Nakajima, R. Tsurutani, J. Chem. Eng. Jpn. 28 (1995) 517–524. (b) L.A. Ryabova, L.M. Vinokurov, E.A. Shekhovtsova, Y.B. Alakhov, A.S. Spirin, Anal. Biochem. 226 (1995) 184–186. (c) R.S. Langer, B.K. Hamilton, C.R. Gardner, M.C. Archer, C.K. Colton, AIChE 22 (1976) 1079–1090.
[33] P.I. Bauer, G. Várady, Anal. Biochem. 91 (1978) 613–617.
[34] (a) R. Kluger, K. Nakaoka, W.-C. Tsui, J. Am. Chem. Soc. 100 (1978) 7388–7392. (b) R. Kluger, K. Nakaoka, Biochemistry 13 (1974) 910–914.
[35] (a) D.B. Olsen, T.W. Hepburn, S.-l. Lee, B.M. Martin, P.S. Mariano, D. Dunaway-Mariano, Arch. Biochem. Biophys. 296 (1992) 144–151. (b) D.B. Olsen, T.W. Hepburn, M. Moos, P.S. Mariano, D. Dunaway-Mariano, Biochemistry 27 (1988) 2229–2234.
[36] (a) V. Massey, J. Biol. Chem. 269 (1994) 22459–22462. (b) S. Ghisla, V. Massey, Eur. J. Biochem. 181 (1989) 1–17. (c) P. Hemmerich, V. Massey, H. Michel, C. Schug, Struct. Bonding (Berlin) 48 (1982) 93–123. (c) C. Walsh, Acc. Chem. Res. 13 (1980) 148–155.
[37] Y. Noguchi, T. Fujiwara, K. Yoshimatsu, Y. Fukumori, J. Bacteriol. 181 (1999) 2142–2147.
[38] J.M. Perry, M.A. Marletta, Proc. Nat. Acad. Sci. USA 95 (1998) 11101–11106.
[39] K. Brunner, A. Tortschanoff, B. Hemmens, P.J. Andrew, B. Mayer, A.J. Kungl, Biochemistry 37 (1998) 17545–17553.
[40] P.J. Andrew, B. Mayer, Cardiovasc. Res. 43 (1999) 521–531.
[41] (a) E.D. Coulter, N. Moon, C.J. Batie, W.R. Dunham, D.P. Ballou, Biochemistry 38 (1999) 11062–11072. (b) D.F. Becker, U. Leartsakulpanich, K.K. Surerus, J.G. Ferry, S.W. Ragsdale, J. Biol. Chem. 273 (1998) 26462–26469. (c) A. Fournel, S. Gambarelli, B. Guigliarelli, C. More, M. Asso, G. Chouteau, R. Hille, P. Bertrand, J. Chem. Phys. 109 (1998) 10905–10913.
[42] (a) K.J. Baek, B.A. Thiel, S. Lucas, D.J. Stuehr, J. Biol. Chem. 268 (1993) 21120–21129. (b) L. Chen, M.-Y. Liu, J. LeGall, Arch. Biochem. Biophys. 303 (1993) 44–50.
[43] H. Sigel, A. Sigel (Eds.), Metal Ions in Biological Systems, vol. 17, Calcium and its Role in Biology, Marcel Dekker, New York and Basel, 1984.
[44] H. Sigel, A. Sigel (Eds.), Metal Ions in Biological Systems, vol. 26, Compendium on Magnesium and Its Role in Biology, Nutrition, and Physiology, Marcel Dekker, New York and Basel, 1990.
[45] A. Sigel, H. Sigel (Eds.), Metal Ions in Biological Systems, vol. 37, Manganese and Its Role in Biological Processes, Marcel Dekker, New York and Basel, 2000.
[46] H. Sigel, A. Sigel (Eds.), Metal Ions in Biological Systems, vol. 15, Zinc and Its Role in Biology and Nutrition, Marcel Dekker, New York and Basel, 1983.
[47] R.B. Martin, H. Sigel, Comments Inorg. Chem. 6 (1988) 285–314.
[48] H. Sigel, S.S. Massoud, R. Tribolet, J. Am. Chem. Soc. 110 (1988) 6857–6865.
[49] H. Sigel, D. Chen, N.A. Corfù, F. Gregáň, A. Holý, M. Strašák, Helv. Chim. Acta 75 (1992) 2634–2656.
[50] S.S. Massoud, H. Sigel, Inorg. Chem. 27 (1988) 1447–1453.
[51] D. Chen, M. Bastian, F. Gregáň, A. Holý, H. Sigel, J. Chem. Soc. Dalton Trans. (1993) 1537–1546.
[52] D. Chen, F. Gregáň, A. Holý, H. Sigel, Inorg. Chem. 32 (1993) 5377–5384.
[53] M. Bastian, D. Chen, F. Gregáň, G. Liang, H. Sigel, Z. Naturforsch. Teil B 48 (1993) 1279–1287.
[54] M.C.F. Magalhães, H. Sigel, J. Indian Chem. Soc. 69 (1992) 437–441.
[55] H. Sigel, Angew. Chem. 87 (1975) 391–400; Angew. Chem. Int. Ed. Engl. 14 (1975) 394–402.
[56] (a) H. Sigel, B.E. Fischer, B. Prijs, J. Am. Chem. Soc. 99 (1977) 4489–4496. (b) H. Sigel, Inorg. Chem. 19 (1980) 1411–1413.
[57] (a) J. Zhao, B. Song, N. Saha, A. Saha, F. Gregáň, M. Bastian, H. Sigel, Inorg. Chim. Acta 250 (1996) 185–188. (b) B. Song, S.A.A. Sajadi, F. Gregáň, N. Prónayová, H. Sigel, Inorg. Chim. Acta 273 (1998) 101–105.
[58] C.A. Blindauer, A. Holý, H. Sigel, Coll. Czech. Chem. Commun. 64 (1999) 613–632.
[59] C.A. Blindauer, A.H. Emwas, A. Holý, H. Dvořáková, E. Sletten, H. Sigel, Chem. Eur. J. 3 (1997) 1526–1536.
[60] C.A. Blindauer, T.I. Sjåstad, A. Holý, E. Sletten, H. Sigel, J. Chem. Soc. Dalton Trans. (1999) 3661–3671.
[61] G. Liang, D. Chen, M. Bastian, H. Sigel, J. Am. Chem. Soc. 114 (1992) 7780–7785.

[62] (a) D.C. Rees, J. Mol. Biol. 141 (1980) 323–326. (b) G.R. Moore, FEBS Lett. 161 (1983) 171–175. (c) N.K. Rogers, G.R. Moore, M.J.E. Sternberg, J. Mol. Biol. 182 (1985) 613–616. (d) S.C. Harvey, Proteins Struct. Funct. Genet. 5 (1989) 78–92. (e) G. Iversen, Y.I. Kharkats, J. Ulstrup, J. Mol. Phys. 94 (1998) 297–306.
[63] (a) H. Sigel, R.B. Martin, R. Tribolet, U.K. Häring, R. Malini-Balakrishnan, Eur. J. Biochem. 152 (1985) 187–193. See also the comment in the footnote on page 258 in: (b) M. Bastian, H. Sigel, Inorg. Chim. Acta 178 (1990) 249–259.
[64] L. De Meis, Biochim. Biophys. Acta 973 (1989) 333–349.
[65] (a) G. Åkerlöf, O.A. Short, J. Am. Chem. Soc. 58 (1936) 1241–1243. (b) F.E. Critchfield, J.A. Gibson, Jr., J.L. Hall, J. Am. Chem. Soc. 75 (1953) 1991–1992. (c) G. Åkerlöf, O.A. Short, J. Am. Chem. Soc. 75 (1953) 6357.
[66] (a) A.R. Plater, S.M. Zgiby, G.J. Thomson, S. Qamar, C.W. Wharton, A. Berry, J. Mol. Biol. 285 (1999) 843–855. (b) B.S. Szwergold, K. Ugurbil, T.R. Brown, Arch. Biochem. Biophys. 317 (1995) 244–252.
[67] P. Karlson, D. Doenecke, G. Fuchs, J. Koolman, G. Schäfer, Kurzes Lehrbuch der Biochemie, 13th ed. Thieme Verlag, Stuttgart and New York, 1988.
[68] (a) B. Plaut, J.R. Knowles, Biochem. J. 129 (1972) 311–320. (b) J.G. Belasco, J.M. Herlihy, J.R. Knowles, Biochemistry 17 (1978) 2971–2978. (c) W.W. Cleland, Adv. Enzymol. 45 (1977) 273–387.
[69] J.R. Knowles, Nature 350 (1991) 121–124.
[70] The Merck Index, 11th ed., No. 4377, Merck, Rahway, NJ, 1989, p. 704.
[71] H. Sigel, C.P. Da Costa, B. Song, P. Carloni, F. Gregáň, J. Am. Chem. Soc. 121 (1999) 6248–6257.
[72] A. Saha, N. Saha, L.-n. Ji, J. Zhao, F. Gregáň, S.A.A. Sajadi, B. Song, H. Sigel, J. Biol. Inorg. Chem. 1 (1996) 231–238.
[73] (a) Cu^{2+}: H. Sigel, R.B. Martin, Chem. Rev. 82 (1982) 385–426. (b) Zn^{2+}: H. Sigel, R.B. Martin, Chem. Soc. Rev. 23 (1994) 83–91.
[74] M. Ushimaru, Y. Shinohara, Y. Fukushima, J. Biochem. 122 (1997) 666–674.
[75] Gmelins Handbuch der Anorganischen Chemie, vol. 8., völlig neu bearbeitete Auflage, Verlag Chemie, Weinheim: (a) Magnesium (Syst.-Nr. 27), Teil A, 1952, p. 172. (b) Calcium (Syst.-Nr. 28), Teil A, 1957, p. 390. (c) Strontium (Syst.-Nr. 29), 1931; p. 40. (d) Barium (Syst.-Nr. 30), 1932, p. 39.
[76] C.P. Da Costa, B. Song, F. Gregáň, H. Sigel, J. Chem. Soc., Dalton Trans (2000) 899–904.
[77] H. Sigel, B. Song, G. Liang, R. Halbach, M. Felder, M. Bastian, Inorg. Chim. Acta 240 (1995) 313–322.
[78] J. Bidwell, J. Thomas, J. Stuehr, J. Am. Chem. Soc. 108 (1986) 820–825.
[79] (a) H. Sigel, S.S. Massoud, N.A. Corfù, J. Am. Chem. Soc. 116 (1994) 2958–2971. (b) H. Sigel, Eur. J. Biochem. 165 (1987) 65–72.
[80] M. Bastian, H. Sigel, J. Coord. Chem. 23 (1991) 137–154.
[81] M. Bastian, H. Sigel, Biophys. Chem. 67 (1997) 27–34.
[82] M. Bastian, H. Sigel, Inorg. Chem. 36 (1997) 1619–1624.
[83] (a) K. Tajima, T. Mizuhata, K. Ishizu, K. Mukai, N. Azuma, Abstracts EuroBIC-II (Metal Ions in Biological Systems), Florence, Italy, 1994, p. 308. (b) K. Aoki, H. Yamazaki, J. Chem. Soc. Dalton Trans. (1987) 2017–2021. (c) M. Sabat, M. Jezowska, H. Kozlowski, Inorg. Chim. Acta 37 (1979) L511–L512. (d) D. van der Helm, C.E. Tatsch, Acta Crystallogr. Sect. B, 28 (1972) 2307–2312.
[84] (a) A. Odani, R. Shimata, H. Masuda, O. Yamauchi, Inorg. Chem. 30 (1991) 2133–2138. (b) O. Yamauchi, A. Odani, T. Kohzuma, H. Masuda, K. Toriumi, K. Saito, Inorg. Chem. 28 (1989) 4066–4068. (c) H. Masuda, O. Matsumoto, A. Odani, O. Yamauchi, Nippon Kagaku Kaishi (1988) 783–788.
[85] H. Sigel, R. MaliniBalakrishnan, U.K. Häring, J. Am. Chem. Soc. 107 (1985) 5137–5148.
[86] G. Liang, H. Sigel, Z. Naturforsch. Teil B 44 (1989) 1555–1566.
[87] H. Sigel, Pure Appl. Chem. 61 (1989) 923–932.
[88] G. Liang, R. Tribolet, H. Sigel, Inorg. Chim. Acta 155 (1989) 273–280.
[89] G. Liang, R. Tribolet, H. Sigel, Inorg. Chem. 27 (1988) 2877–2887.
[90] H. Sigel, A. Saha, N. Saha, P. Carloni, L.E. Kapinos, R. Griesser, J. Inorg. Biochem. 78 (2000) 129–137.
[91] G. Liang, H. Sigel, Inorg. Chem. 29 (1990) 3631–3632.